ENZYMEFLOW: GENERATING REACTION-SPECIFIC ENZYME CATALYTIC POCKETS THROUGH FLOW MATCHING AND CO-EVOLUTIONARY DYNAMICS

Anonymous authors
Paper under double-blind review

ABSTRACT

Enzyme design is a critical area in biotechnology, with applications ranging from drug development to synthetic biology. Traditional methods for enzyme function prediction or protein binding pocket design often fall short in capturing the dynamic and complex nature of enzyme-substrate interactions, particularly in catalytic processes. To address the challenges, we introduce EnzymeFlow, a generative model that employs flow matching with hierarchical pre-training and enzyme-reaction co-evolution to generate catalytic pockets for specific substrates and catalytic reactions. Additionally, we introduce a large-scale, curated, and validated dataset of enzyme-reaction pairs, specifically designed for the catalytic pocket generation task, comprising a total of $328,192$ pairs. By incorporating evolutionary dynamics and reaction-specific adaptations, EnzymeFlow becomes a powerful model for designing enzyme pockets, which is capable of catalyzing a wide range of biochemical reactions. Experiments on the new dataset demonstrate the model's effectiveness in designing high-quality, functional enzyme catalytic pockets, paving the way for advancements in enzyme engineering and synthetic biology. The EnzymeFlow code can be found at `https://anonymous.4open.science/r/EnzymeFlow-7420`.

1 INTRODUCTION

Proteins are fundamental to life, participating in many essential interactions for biological processes (Whitford, 2013). Among proteins, enzymes stand out as a specialized class that serves as catalysts, driving and regulating nearly all chemical reactions and metabolic pathways across living organisms, from simple bacteria to complex mammals (Kraut, 1988; Murakami et al., 1996; Copeland, 2023) (visualized in Fig. 1). Their catalytic power is central to biological functions, enabling the efficient production of complex organic molecules in biosynthesis (Ferrer et al., 2008; Liu & Wang, 2007) and the creation of novel biological pathways in synthetic biology (Girvan & Munro, 2016; Keasling, 2010; Hodgman & Jewett, 2012). Examining enzyme functions across the tree of life deepens our understanding of the evolutionary processes that shape metabolic networks and enable organisms to adapt to their environments (Jensen, 1976; Glasner et al., 2006; Campbell et al., 2016; Pinto et al., 2022). Consequently, studying enzyme-substrate interactions is essential for comprehending biological processes and designing effective products.

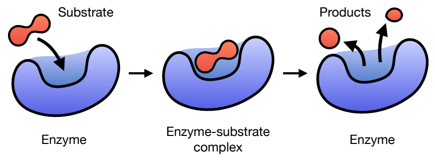

Figure 1: Enzyme-substrate Mechanism.

Traditional methods have primarily focused on enzyme function prediction, annotation (Gligorijević et al., 2021; Yu et al., 2023), or enzyme-reaction retrieval (Mikhael et al., 2024; Hua et al., 2024b; Yang et al., 2024). These approaches lack the ability to design new enzymes that catalyze specific biological processes. Recent studies suggest that current function prediction models struggle to generalize to unseen enzyme reaction data (de Crecy-Lagard et al., 2024; Kroll et al., 2023a), limiting their utility in enzyme design. To effectively design enzymes, it is crucial not only to predict protein functions but also to identify and generate enzyme catalytic pockets specific to particular substrates and reactions, thereby enabling potentially valuable biological processes.

On the other hand, recent advances in deep generative models have significantly improved pocket design for protein-ligand complexes (Stärk et al., 2023; Zhang et al., 2023b; 2024d; Krishna et al., 2024), generating diverse and functional binding pockets for ligand molecules. However, these models cannot generalize directly to the design of enzyme catalytic pockets for substrates involved in catalytic processes. Unlike protein-ligand complexes, where ligand binding typically does not lead to a chemical transformation, **enzyme-substrate interactions result in a chemical change where the substrate is converted into a product,** which has significantly different underlying mechanisms. More specifically, in protein-ligand binding, the ligand may induce a conformational change in the protein, affect its interactions with other molecules, or modulate its activity; in contrast, the formation of an enzyme-substrate complex is a precursor to a catalytic reaction, where the enzyme lowers the activation energy, facilitating the transformation of the substrate into a product. After the reaction, the enzyme is free to catalyze another substrate molecule. Therefore, current generative models for pocket design are restricted and limited to static ligand-binding interactions, failing to describe such dynamic transformations and the complex nature of enzyme-substrate interactions.

To address these limitations, we propose EnzymeFlow (demonstrated in Fig. 3), a flow matching model (Lipman et al., 2022; Liu et al., 2022; Albergo & Vanden-Eijnden, 2023) with enzyme-reaction co-evolution and structure-based pre-training for enzyme catalytic pocket generation. Our major contributions follow: **(1) EnzymeFlow—Flow Model for Enzyme Catalytic Pocket Design:** We define conditional flows for enzyme catalytic pocket generation based on backbone frames, amino acid types, and Enzyme Commission (EC) class. The generative flow process is conditioned on specific substrates and products, enabling potential catalytic processes. **(2) Enzyme-Reaction Co-Evolution:** Since enzyme-substrate interactions involve dynamic chemical transformations of substrate molecules, which is distinct from static protein-ligand interactions, we propose enzyme-reaction co-evolution with a new co-evolutionary transformer (*coEvoFormer*). The co-evolution is used to capture substrate-specificity in catalytic reactions. It encodes how enzymes and reactions evolve together, allowing the model to operate on evolutionary dynamics, which naturally comprehends the catalytic process. **(3) Structure-Based Hierarchical Pre-Training:** To leverage the vast data of geometric structures from existing proteins and protein-ligand complexes, we propose a structure-based hierarchical pre-training. This method progressively learns from protein backbones to protein binding pockets, and finally to enzyme catalytic pockets. This hierarchical learning of protein structures enhances geometric awareness within the model. **(4) EnzymeFill—Large-scale Pocket-specific Enzyme-Reaction Dataset with Pocket Structures:** Current enzyme-reaction datasets are based on full enzyme sequences or structures and lack precise geometry for how enzyme pockets catalyze the substrates. To address this, we construct a structure-based, curated, and validated enzyme catalytic pocket-substrate dataset, specifically designed for the catalytic pocket generation task.

2 Related Work

2.1 Protein Evolution

Protein evolution learns how proteins change over time through processes such as mutation, selection, and genetic drift (Pál et al., 2006; Bloom & Arnold, 2009), which influence protein functions. Studies on protein evolution focus on understanding the molecular mechanisms driving changes in protein sequences and structures. Zuckerkandl & Pauling (1965) introduce the concept of the molecular clock, which postulates that proteins evolve at a relatively constant rate over time, providing a framework for estimating divergence times between species. DePristo et al. (2005) show that evolutionary rates are influenced by functional constraints, with regions critical to protein function (*e.g.*, active sites, binding interfaces) evolving more slowly due to purifying selection. This understanding leads to the development of methods for detecting functionally important residues based on evolutionary conservation. Understanding protein evolution has practical applications in protein engineering. By studying how natural proteins evolve to acquire new functions, researchers design synthetic proteins with desired properties (Xia & Levitt, 2004; Jäckel et al., 2008). Additionally, deep learning models increasingly integrate evolutionary principles to predict protein function and stability, design novel enzymes, and guide protein engineering (Yang et al., 2019; AlQuraishi, 2019; Jumper et al., 2021).

2.2 Generative Models for Protein and Pocket Design

Recent advancements in generative models have advanced the field of protein design and binding pocket design, enabling the creation of proteins or binding pockets with desired properties and functions (Yim et al., 2023a;b; Chu et al., 2024; Hua et al., 2024a; Abramson et al., 2024). For example, RFDiffusion (Watson et al., 2023) employs denoising diffusion in conjunction with RoseTTAFold (Baek et al., 2021) for *de novo* protein structure design, achieving wet-lab-level generated structures that can be extended to binding pocket design. RFDiffusionAA (Krishna et al., 2024) extends RFDiffusion for joint modeling of protein and ligand structures, generating ligand-binding proteins and further leveraging MPNNs for sequence design. Additionally, FAIR (Zhang et al., 2023b) and

PocketGen (Zhang et al., 2024d) use a two-stage coarse-to-fine refinement approach to co-design pocket structures and sequences. Recent models leveraging flow matching frameworks have shown promising results in these tasks. For instance, FoldFlow (Bose et al., 2023) introduces a series of flow models for protein backbone design, improving training stability and efficiency. FrameFlow (Yim et al., 2023a) further enhances sampling efficiency and demonstrates success in motif-scaffolding tasks using flow matching, while MultiFlow (Campbell et al., 2024) advances to structure and sequence co-design. These flow models, initially applied to protein backbones, have been further generalized to binding pockets. For example, PocketFlow (Zhang et al., 2024e) combines flow matching with physical priors to explicitly learn protein-ligand interactions in binding pocket design, achieving stronger results compared to RFDiffusionAA. While these models excel in protein and binding pocket design, they primarily focus on static protein(-ligand) interactions and lack the ability to model the chemical transformations involved in enzyme-catalyzed reactions. This limitation may reduce their accuracy and generalizability in designing enzyme pockets for catalytic reactions. In EnzymeFlow, we aim to address these current limitations. An extended discussion of related works on AI-driven protein engineering can be found in App. C.

Discussion regarding PocketFlow. PocketFlow (Zhang et al., 2024e) has demonstrated strong performance in protein-ligand design, showing generalizability across various protein pocket categories. However, it falls short when applied to the design of enzyme catalytic pocket with specific substrates. One key limitation is that protein-ligand interactions are static, meaning that the training data and model design do not capture or describe the chemical transformations, such as the conversion or production of new molecules, that occur during enzyme-catalyzed reactions. This dynamic aspect of enzyme-substrate interactions is missing in current models. Another limitation is that PocketFlow fixes the overall protein backbone structure before designing the binding pocket, treating the pocket as a missing element to be filled in. This approach may not align with practical needs, as the overall protein backbone structure is often unknown before pocket design. Ideally, the design process should be reversed: the pocket should be designed first, influencing the overall protein structure. Despite these challenges, PocketFlow remains a good and leading work in pocket design. With EnzymeFlow, we aim to address these limitations, particularly in the context of catalytic pocket design.

3 EnzymeFill: Large-scale Enzyme Pocket-Reaction Dataset

A key limitation of current datasets, such as ESP (Kroll et al., 2023b), EnzymeMap (Heid et al., 2023), CARE (Yang et al., 2024), or ReactZyme (Hua et al., 2024b), is the lack of precise pocket information. These datasets typically provide enzyme-reaction data, including protein sequences and SMILES representations, which is used to predict EC numbers in practice. To address it, we introduce a new synthetic dataset, EnzymeFill, which includes precise pocket structures with substrate conformations. EnzymeFill is specifically introduced for enzyme catalytic pocket design.

Data Source. We construct a curated and validated dataset of enzyme-reaction pairs by collecting data from the Rhea (Bansal et al., 2022), MetaCyc (Caspi et al., 2020), and Brenda (Schomburg et al., 2002) databases. For enzymes in these databases, we exclude entries missing UniProt IDs or protein sequences. For reactions, we apply the following procedures: (1) remove cofactors, small ion groups, and molecules that appear in both substrates and products within a single reaction; (2) exclude reactions with more than five substrates or products; and (3) apply OpenBabel (O'Boyle et al., 2011) to standardize canonical SMILES. Ultimately, we obatin a total of $328,192$ enzyme-reaction pairs, comprising $145,782$ unique enzymes and $17,868$ unique reactions; we name it EnzymeFill.

Catalytic Pocket with AlphaFill. We identify all enzyme catalytic pockets using AlphaFill (Hekkelman et al., 2023), an AF-based algorithm that uses sequence and structure similarity to transplant ligand molecules from experimentally determined structures to predicted protein models. We download the AlphaFold structures for all enzymes and apply AlphaFill to extract the enzyme pockets. Simultaneously, we determine the reaction center by using atom-atom mapping of the reactions. During the pocket extraction process, AlphaFill first identifies homologous proteins of the target enzyme in the PDB-REDO database, along with their complexes with ligands (van Beusekom et al., 2018). It then transplants the ligands from the homologous protein complexes to the target enzyme through structural alignment (illustrated in Fig. 2(a)). After transplantation, we select the appropriate ligand molecule based on the number of atoms and its frequency of occurrence, and extract the pocket using a pre-defined radius of $10\mathring{A}$. We also perform clustering analysis on the extracted pockets using Foldseek (van Kempen et al., 2022), which reveals that enzyme catalytic pockets capture functional information more effectively than full structures (illustrated in Fig. 2(b)). For the extraction of

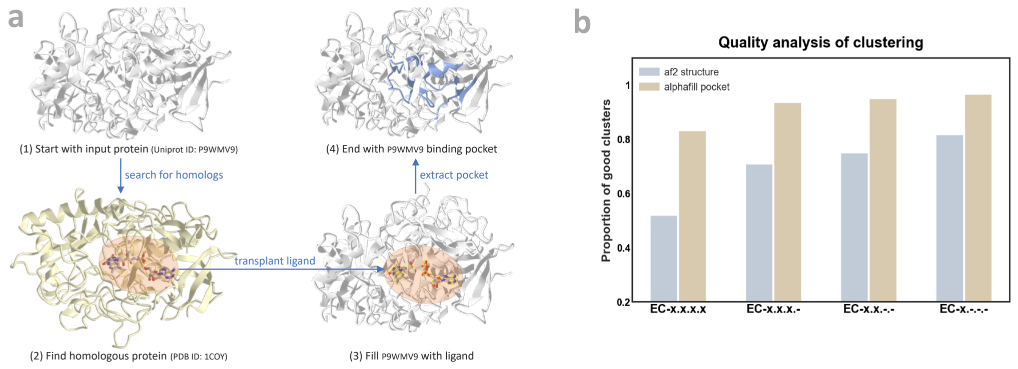
a
(1) Start with input protein (Uniprot ID: P9WMV9)
search for homologs
(2) Find homologous protein (PDB ID: 1COY)
transplant ligand
(3) Fill P9WMV9 with ligand
extract pocket
(4) End with P9WMV9 binding pocket
b
Quality analysis of clustering
af2 structure
alphafill pocket
Proportion of good clusters
0.2
0.4
0.6
0.8
1
EC-x.x.x.x
EC-x.x.x.-
EC-x.x.-.-
EC-x.-.-.-

Figure 2: **(a)** Enzyme pocket extraction workflow with AlphaFill. **(b)** Quality analysis of clustering between enzyme pockets and full structures; good clusters have high functional concentration.

reaction centers, we first apply RXNMapper to extract atom-atom mappings (Schwaller et al., 2021), which maps the atoms between the substrates and products. We then identify atoms where changes occurred in chemical bonds, charges, and chirality, labeling these atoms as reaction centers.

Data Debiasing for Generation. To ensure the quality of catalytic pocket data for the design task, we exclude pockets with fewer than 32 residues[1], resulting in $232,520$ enzyme-reaction pairs. Additionally, enzymes and their catalytic pockets can exhibit significant sequence similarity. When enzymes that are highly similar in sequence appear too frequently in the dataset, they tend to belong to the same cluster or homologous group, which can introduce substantial biases during model training. To mitigate this issue and ensure a more balanced dataset, it is important to reduce the number of homologous enzymes by clustering and selectively removing enzymes from the same clusters. This helps to debias the data and improve the model's generalizability. We perform sequence alignment to cluster enzymes and identify homologous ones (Steinegger & Söding, 2017). We then revise the dataset into five major categories based on enzyme sequence similarity, resulting in: (1) $19,379$ pairs with at most 40% homology, (2) $34,750$ pairs with at most 50% homology, (3) $53,483$ pairs with at most 60% homology, (4) $100,925$ pairs with at most 80% homology, and (5) $132,047$ pairs with at most 90% homology. In EnzymeFlow, we choose to use the clustered data with at most 60% homology with $53,483$ samples for training. We provide more dataset statistics in App. H

4 EnzymeFlow

We introduce EnzymeFlow, a flow matching model with hierarchical pre-training and enzyme-reaction co-evolution for enzyme catalytic pocket design, conditioned on specific catalytic reactions and trained on EnzymeFill. We demonstrate the pipeline in Fig. 3, discuss the EnzymeFlow with co-evolution in Sec. 4.1, further introduce the structure-based hierarchical pre-training in Sec. 4.2.

4.1 Enzyme Catalytic Pocket Generation with Flow Matching

EnzymeFlow on Catalytic Pocket. Following Yim et al. (2023a), we refer to the protein structure as the backbone atomic coordinates of each residue. A pocket with number of residues N_r can be parameterized into SE(3) residue frames $\{(x^i, r^i, c^i)\}_{i=1}^{N_r}$, where $x^i \in \mathbb{R}^3$ represents the position (translation) of the C_α atom of the i-th residue, $r^i \in$ SO(3) is a rotation matrix defining the local frame relative to a global reference frame, and $c^i \in \{1, \ldots, 20\} \cup \{\times\}$ denotes the amino acid type, with an additional $\times$ indicating a *masking state* of the amino acid type. We refer to the residue block as $T^i = (x^i, r^i, c^i)$, and the entire pocket is described by a set of residues $\mathbf{T} = \{T^i\}_{i=1}^{N_r}$. Additionally, we denote the graph representations of substrate and product molecules in the catalytic reaction as l_s and l_p, respectively. An enzyme-reaction pair can therefore be described as $(\mathbf{T}, l_s, l_p)$.

Following flow matching literature (Yim et al., 2023a; Campbell et al., 2024), we use time $t = 1$ to denote the source data. The conditional flow on the enzyme catalytic pocket $p_t(\mathbf{T}_t|\mathbf{T}_1)$ for a time step $t \in (0, 1]$ can be factorized into the probability density over continuous variables (translations and rotations) and the probability mass function over discrete variables (amino acid types) as:

$$p_t(\mathbf{T}_t|\mathbf{T}_1) = \prod_{i=1}^{N_r} p_t(x_t^i|x_1^i)\; p_t(r_t^i|r_1^i)\; p_t(c_t^i|c_1^i), \tag{1}$$

[1]32 residues are chosen based on LigandMPNN (Dauparas et al., 2023), ensuring high-quality interactions.

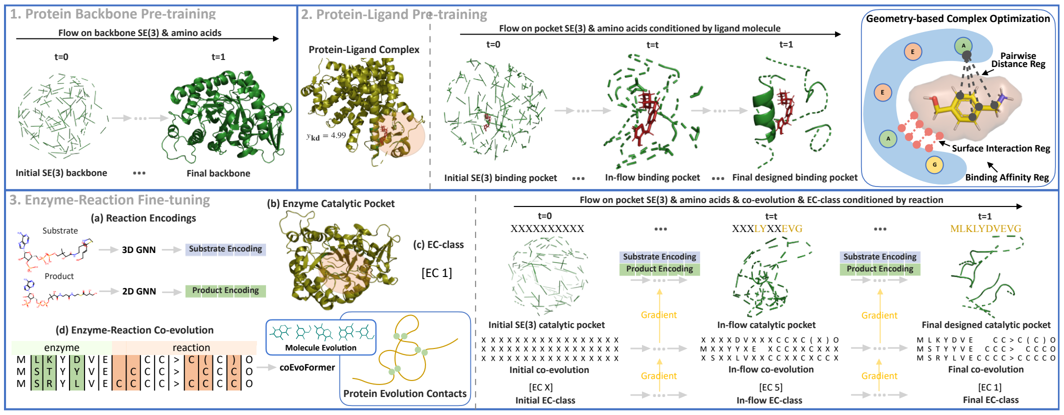
1. Protein Backbone Pre-training
Flow on backbone SE(3) & amino acids
t=0
t=1
Initial SE(3) backbone
Final backbone
2. Protein-Ligand Pre-training
Protein-Ligand Complex
Flow on pocket SE(3) & amino acids conditioned by ligand molecule
Initial SE(3) binding pocket
In-flow binding pocket
Final designed binding pocket
Geometry-based Complex Optimization
Pairwise Distance Reg
Surface Interaction Reg
Binding Affinity Reg
3. Enzyme-Reaction Fine-tuning
(a) Reaction Encodings
Substrate
Product
3D GNN
2D GNN
Substrate Encoding
Product Encoding
(b) Enzyme Catalytic Pocket
(c) EC-class
[EC 1]
(d) Enzyme-Reaction Co-evolution
enzyme
reaction
Molecule Evolution
coEvoFormer
Protein Evolution Contacts
Flow on pocket SE(3) & amino acids & co-evolution & EC-class conditioned by reaction
Initial SE(3) catalytic pocket
In-flow catalytic pocket
Final designed catalytic pocket
Gradient
Initial co-evolution
In-flow co-evolution
Final co-evolution
[EC X]
Initial EC-class
[EC 5]
In-flow EC-class
Final EC-class
XXXXXXXXXX
XXXLYXXEVG
MLKLYDVEVG

Figure 3: Overview of EnzymeFlow with hierarchical pre-training and enzyme-reaction co-evolution. **(1)** Flow model pre-trained on protein backbones and amino acid types. **(2)** Flow model further pre-trained on protein binding pockets, conditioned on ligand molecules with geometry-specific optimization. **(3)** Flow model fine-tuned on enzyme catalytic pockets, and conditioned on substrate and product molecules, with enzyme-reaction co-evolution and EC-class generation.

where the translation, rotation, and amino acid type at time t are derived as:

$$\begin{aligned} &x_t^i = (1-t)x_0^i + tx_1^i,\ x_0^i \sim \mathcal{N}(0, I);\ \ r_t^i = \exp_{r_0^i}(t \log_{r_0^i} r_1^i),\ r_0^i \sim \mathcal{U}_{\mathrm{SO(3)}};\\ &c_t^i \sim p_t(c_t^i|c_1^i) = \mathrm{Cat}(t\,\delta(c_1^i, c_t^i) + (1-t)\,\delta(\times, c_t^i)), \end{aligned} \tag{2}$$

where $\delta(\mathrm{a}, \mathrm{b})$ is the Kronecker delta, which equals to 1 if $\mathrm{a} = \mathrm{b}$ and 0 if $\mathrm{a} \neq \mathrm{b}$; Cat is a categorical distribution for the sampling of discrete amino acid type, with probabilities $t\delta(c_1^i, c_t^i) + (1-t)\delta(\times, c_t^i)$. The discrete flow interpolates from the *masking state* $\times$ at $t = 0$ to the actual amino acid type c_1^i at $t = 1$ (Campbell et al., 2024). In a catalytic process, enzymes interact with substrates to produce specific products. In practical enzyme design, we typically know the substrates l_s (as 3D atom point clouds) and the desired products l_p (as 2D molecular graphs or SMILES). Therefore, the formation of the enzyme catalytic pocket should be conditioned on both substrates and products. Our enzyme flow matching model is conditioned on these two ligand molecules l_s, l_p, ensuring that the predictions of vector fields $v_\theta(\cdot)$ and loss functions account for the substrate and product molecules:

$$\begin{aligned} &\mathcal{L}_{\text{trans}} = \sum_{i=1}^{N_r} \|v_\theta^i(x_t^i, t, l_s, l_p) - (x_1^i - x_0^i)\|_2^2;\ \mathcal{L}_{\text{rot}} = \sum_{i=1}^{N_r} \|v_\theta^i(r_t^i, t, l_s, l_p) - \frac{\log_{r_t^i} r_1^i}{1-t}\|_{\mathrm{SO(3)}}^2;\\ &\mathcal{L}_{\text{aa}} = -\sum_{i=1}^{N_r} \log p_\theta(c_1^i | v_\theta^i(c_t^i, t, l_s, l_p)). \end{aligned} \tag{3}$$

To design the enzyme pocket and model protein-ligand interactions, we implement 3D and 2D GNNs to encode the substrate and product, respectively (implemented in App. E). The main vector field network applies cross-attention to model protein-ligand interactions and incorporates Invariant Point Attention (IPA) (Jumper et al., 2021) to encode protein features and make predictions. Following tricks in Yim et al. (2023a); Campbell et al. (2024), we let the the model predict the final structure at $t = 1$ and interpolates to compute the vector fields (discussed in App. F).

EnzymeFlow on EC-Class. The Enzyme Commission (EC) classification is crucial for categorizing enzymes based on the reactions they catalyze. Understanding the EC-class of an enzyme-reaction pair can help predict its function in various biochemical pathways (Bansal et al., 2022). Given its importance, EnzymeFlow leverages EC-class to enhance its generalizability across various enzymes and catalytic reactions. Therefore, our model incorporates EC-class, $y_{\text{ec}} \in \{1, \ldots, 7\} \cup \{\times\}$, as a discrete factor in the design process. The EC-class is sampled from a Categorical distribution with probabilities $t\delta(y_{\text{ec}_1}, y_{\text{ec}_t}) + (1-t)\delta(\times, y_{\text{ec}_t})$. The discrete flow on EC-class interpolates from the *masking state* $\times$ at $t = 0$ to the actual EC-class y_{ec_1} at $t = 1$. The prediction and loss function are conditioned on the pocket frames and the substrate and product molecules:

$$\mathcal{L}_{\text{ec}} = -\log p_\theta(y_{\text{ec}_1} | v_\theta(\mathbf{T}_t, t, l_s, l_p, y_{\text{ec}_t})). \tag{4}$$

The model predicts the final EC-class at $t = 1$ and interpolates to compute its vector field. For EC-class prediction, we first employ a EC-class embedding network to encode y_{ec_t}. The final predicted EC-class is obtained by pooling cross-attention between the encoded enzyme and EC-class features.

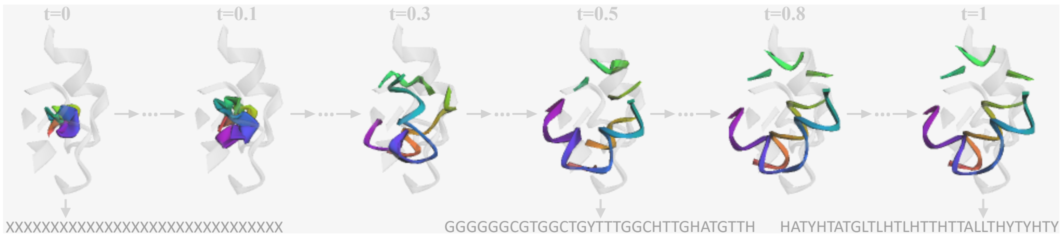
t=0
t=0.1
t=0.3
t=0.5
t=0.8
t=1
XXXXXXXXXXXXXXXXXXXXXXXXXXXXXXXX
GGGGGGCGTGGCTGYTTTGGCHTTGHATGTTH
HATYHTATGLTLHTLHTTHTTALLTHYTYHTY

Figure 4: Catalytic pocket design example using EnzymeFlow (UniProt: Q7U4P2). The pocket generation is conditioned on reaction `CN[C@H](C(=O)C)CS.C/C=C\\1/C(=C/c2[nH]c(c(c2C)CCC(=O)O)/C=C/2\\N=C(C(=C2CCC(=O)O)C)C[C@H]2NC(=O)C(=C2C)C=C)/NC(=O)[C@@H]1C` $\rightarrow$ `CN[C@H](C(=O)C)CSC(C1=C(C)C(=O)N[C@H]1Cc1[nH]c(c(c1C)CCC(=O)O)/C=C/1\\N=C(C(=C1CCC(=O)O)C)C[C@H]1NC(=O)C(=C1C)C=C)C` of EC4 (ligase enzyme), from $t = 0$ to $t = 1$.

4.1.1 EnzymeFlow with Enzyme-reaction co-Evolution

Enzyme (protein) evolution refers to the process by which enzyme structures and functions change over time due to genetic variations, such as mutations, duplications, and recombinations. These changes can lead to alterations in amino acids, potentially affecting the enzyme structure, function, stability, and interactions (Pál et al., 2006; Sikosek & Chan, 2014). Reaction evolution, on the other hand, refers to the process by which chemical reactions or substrates, particularly those catalyzed by enzymes, change and diversify within biological systems over time (illustrated in Fig. 3(3)(d)).

Co-Evolutionary Dynamics. Enzymes can co-evolve with the metabolic or biochemical pathways they are part of, adapting to changes in substrate availability, the introduction of new reaction steps, or the need for more efficient flux through the pathway. As pathways evolve, enzymes within them may develop new catalytic functions or refine existing ones to better accommodate these changes (Noda-Garcia et al., 2018). This process frequently involves the co-evolution of enzymes and their substrates. As substrates change—whether due to the introduction of new compounds in the environment or mutations in other metabolic pathways—enzymes may adapt to catalyze reactions with these new substrates, leading to the emergence of entirely new reactions. Understanding enzyme-substrate interactions, therefore, requires considering their evolutionary dynamics, as these interactions are shaped by the evolutionary history and adaptations of both enzymes and their substrates. This co-evolutionary process is crucial for explaining how enzymes develop new functions and maintain efficiency in response to ongoing changes in their biochemical environment.

To capture the evolutionary dynamics, we introduce the concept of enzyme-reaction co-evolution into EnzymeFlow. We compute the enzyme and reaction evolution by applying multiple sequence alignment (MSA) to enzyme sequences and reaction SMILES, respectively (Steinegger & Söding, 2017). The co-evolution of an enzyme-reaction pair is represented by a matrix $U \in \mathbb{R}^{N_{\text{MSA}} \times N_{\text{token}}}$, which combines the MSA results of enzyme sequences and reaction SMILES (illustrated in Fig. 3(3)(d) & Fig. 9), where N_{MSA} denotes the number of MSA sequences and N_{token} denotes the length of the MSA alignment preserved. And each element $u^{mn} \in \{1, \dots, 64\} \cup \{\times\}$ in U denotes a tokenized character from our co-evolution vocabulary, with additional $\times$ indicating the *masking state*.

EnzymeFlow on Co-Evolution. The flow for co-evolution follows a similar approach to that used for amino acid types and EC-class, treating it as a discrete factor in the design process. The co-evolution is sampled from a Categorical distribution, where each element has probabilities $t\delta(u_1^{mn}, u_t^{mn}) + (1 - t)\delta(\times, u_t^{mn})$. Each element flows independently, reflecting the natural independence of amino acid mutations (Boyko et al., 2008). The discrete flow on co-evolution interpolates from the *masking state* $\times$ at $t = 0$ to the actual character u_1^{mn} at $t = 1$. The prediction and loss function are conditioned on the pocket frames and the substrate and product molecules:

$$\mathcal{L}_{\text{coevo}} = -\sum_{m=1}^{N_{\text{MSA}}} \sum_{n=1}^{N_{\text{token}}} \log p_\theta(u_1^{mn} | v_\theta(\mathbf{T}_t, t, l_s, l_p, u_t^{mn})). \tag{5}$$

The model predicts the final co-evolution at $t = 1$ and interpolates to compute its vector field. For co-evolution prediction, we first introduce a co-evolutionary MSA transformer (coEvoFormer) to encode U_t (implemented in App. D). The final predicted co-evolution is obtained by computing cross-attention between the encoded enzyme and ligand, and the encoded co-evolution features.

We can therefore express EnzymeFlow with co-evolutionary dynamics for catalytic pocket design as:

$$p_t(\mathbf{T}_t, U_t, y_{\text{ec}_t} | \mathbf{T}_1, U_1, y_{\text{ec}_1}, l_s, l_p) = p_t(y_{\text{ec}_t} | y_{\text{ec}_1}, \mathbf{T}_t)\, p_t(U_t | U_1, \mathbf{T}_t)\, p_t(\mathbf{T}_t | \mathbf{T}_1, l_s, l_p). \tag{6}$$

The final EnzymeFlow model performs flows on protein backbones, amino acid types, EC-class, and enzyme-reaction co-evolution. Given the SE(3)-invariant prior and the main SE(3)-equivariant network in EnzymeFlow, the pocket generation process is also SE(3)-equivariant (proven in App. G).

4.2 Structure-based Hierarchical Pre-training

In addition to the standard EnzymeFlow for enzyme pocket design, we propose a hierarchical pre-training strategy to enhance the generalizability of the model across different enzyme categories. The term *hierarchical pre-training* is used because the approach first involves training the flow model to understand protein backbone generation, followed by training it to learn the geometric relationships between proteins and ligand molecules, which form protein binding pockets. After the flow model learns these prior knowledge, we fine-tune it specifically on an enzyme-reaction dataset to generate enzyme catalytic pockets. The term *hierarchical* reflects the progression from protein backbone generation, to protein binding pocket formation, and finally to enzyme catalytic pocket generation.

Specifically, we begin by pre-training the flow model on a protein backbones. Once the model learns it, we proceed to post-train it on a protein-ligands, with the objective of generating binding pockets conditioned on the ligand molecules. Finally, the model is fine-tuned on our EnzymeFlow dataset to generate valid enzyme catalytic pockets for specific substrates and catalytic reactions.

4.2.1 Protein Backbone Pre-training

The initial step involves pre-training the model on a protein backbone dataset (illustrated in Fig. 3(1)). We use the backbone dataset discussed in FrameFlow (Yim et al., 2023a). This pre-training focuses solely on SE(3) backbone frames and discrete amino acid types, allowing the flow model to acquire foundational knowledge of protein backbone geometry and structure.

4.2.2 Protein-Ligand Pre-training

Following the protein backbone pre-training, we proceed to pre-train the flow model on a protein-ligand dataset (illustrated in Fig. 3(2)). Specifically, we use PDBBind2020 (Wang et al., 2004). This pre-training focuses on binding pocket frames, with the flow model conditioned on the 3D representations of ligand molecules l consisting of N_l atoms. Additionally, binding affinity $y_{\text{kd}} \in \mathbb{R}$ and atomic-level pocket-ligand distance $D^i \in \mathbb{R}^{4\times N_l}$ for the i-th residue frame serve as optimization factors. The parametrization is similar to Eq. 6, with conditioning on the ligand molecule as follows:

$$p_t(\mathbf{T}_t, y_{\text{kd}}|\mathbf{T}_1, l) = p_t(y_{\text{kd}}|\mathbf{T}_t, l)\; p_t(\mathbf{T}_t|\mathbf{T}_1, l). \tag{7}$$

In addition to the flow matching losses in Eq. 3, we introduce a loss of protein-ligand interaction to prevent the collision during the binding in generation process. Conceptually, this ensures that the generated pocket atoms do not come into contact with the surface of the ligand molecule. Following previous work on protein-ligand binding (Lin et al., 2022), the surface of a ligand $\{a_j | j \in \mathbb{N}(N_l)\}$is defined as $\{a \in \mathbb{R}^3 | S(a) = \gamma\}$, where $S(a) = -\rho \log(\sum_{j=1}^{N_l} \exp(-|a - a_j|^2/\rho))$. The interior of the ligand molecule is thus defined by $\{a \in \mathbb{R}^3 | S(a) < \gamma\}$, and the binding pocket atoms are constrained to lie within $\{a \in \mathbb{R}^3 | S(a) > \gamma\}$. We also introduce a protein-ligand distance loss to regularize pairwise atomic distances, along with a binding affinity loss to enforce the generation of more valid protein-ligand pairs. These objectives are defined as follows:

$$\mathcal{L}_{\text{inter}} = \sum_{i=1}^{N_r} \max(0, \gamma - S(\hat{A}_t^i)),\; \mathcal{L}_{\text{dist}} = \sum_{i=1}^{N_r} \frac{\|\mathbf{1}\{D_1^i < 8\text{Å}\}(D_1^i - \hat{D}_t^i)\|_2^2}{\sum \mathbf{1}_{D_1^i < 8\text{Å}}},\; \mathcal{L}_{\text{kd}} = \|y_{\text{kd}} - \hat{y}_{\text{kd}}\|^2, \tag{8}$$

where $\hat{A}^i \in \mathbb{R}^{4\times 3}$ denotes the predicted atomic positions of i-th residue frame, $\gamma = 6$ and $\rho = 2$ are hyperparameters, and $\hat{y}_{\text{kd}}$ is the predicted binding affinity for a generated pair. $\hat{D}^i \in \mathbb{R}^{4\times N_l}$ is defined similarly to D^i , based on the distance between the predicted atomic positions and ligand positions for the i-th residue frame. The predicted affinity $\hat{y}_{\text{kd}}$ is obtained by pooling the encoded protein and ligand features. These additional losses are incorporated to improve the model's generalizability, enforcing more constrained geometries for more valid protein pocket design.

5 Experiment — Generating Catalytic Pocket conditioned on Reactions and Substrates

EnzymeFlow is essentially a *function-based* protein design model, where the intended function is defined by the reaction the enzyme will catalyze. Here, we demonstrate that EnzymeFlow outperforms current *structure-based* substrate-conditioned protein design models in both the structural and functional aspects, showing its capability and advantage in enzyme catalytic pocket design.

Table 1: EnzymeFlow Evaluation Data Statistics.

Data	Pair	Enzyme	Substrate		Product		Enzyme Commision						
	#pair	#enzyme	#substrate	#avg atom	#product	#avg atom	EC1	EC2	EC3	EC4	EC5	EC6	EC7
Raw	232520	97912	7259	30.81	7664	30.34	44881 (19.30)	75944 (32.66)	37728 (16.23)	47242 (20.32)	8315 (3.58)	18281 (7.86)	129 (0.06)
Train	53483	22350	6112	30.95	6331	30.34	11674 (21.83)	18419 (34.44)	11394 (21.30)	5555 (10.39)	2194 (4.10)	4200 (7.85)	47 (0.09)
Eval	100	100	100	30.7	94	28.84	17 (17.00)	17 (17.00)	17 (17.00)	17 (17.00)	16 (16.00)	16 (16.00)	0 (0.00)

We compare EnzymeFlow with state-of-the-arts representative baselines, including template-matching method DEPACT (Chen et al., 2022), deep equivariant and iterative refinement model PocketGen (Zhang et al., 2024d), golden-standard diffusion model RFDiffusionAA (Krishna et al., 2024), and the most recent PocketFlow[2] (Zhang et al., 2024e). For RFDiffusionAA-designed pockets, we apply LigandMPNN (Dauparas et al., 2023) to inverse fold and predict the sequences post-hoc. We provide EnzymeFlow code at `https://anonymous.4open.science/r/EnzymeFlow-7420`.

Evaluation Data. We use MMseqs2 to perform clustering with a 10% homology threshold, selecting the center of each cluster as the initial dataset, resulting in a total of $3,417$ pairs. After de-duplicating both repeated substrates and UniProt entries, we are left with 839 unique enzyme-reaction pairs. We then uniformly sample data across different EC classes, selecting 17 pairs from EC1 to EC4 classes and 16 pairs from EC5 and EC6 classes, respectively, resulting in a total of 100 unique catalytic pockets and 100 unique reactions. Each enzyme-reaction pair is labeled with a ground-truth EC-class from EC1 to EC6. We present the EC-class distribution in the evaluation set in Tab. 1.

Reaction-conditioned Generation. For pocket design and model sampling, we perform conditional generation on each reaction (or substrate), generating 100 catalytic pockets for each reaction in the evaluation set. We evaluate the generated pockets for their structures and functions (*i.e.,* EC-class).

5.1 Catalytic Pocket Structure Evaluation

We begin by assessing the structural validity of generated catalytic pockets. While enzyme function determines whether the designed pocket can catalyze a specific reaction, the structure determines whether the substrate conformation can properly bind to the catalytic pocket. We provide some visual examples of designed pockets in Fig. 5 and Fig. 14.

Metrics. We use the following metrics to evaluate and compare the structural validity of the generated pockets. Constrained-site RMSD (`cRMSD`): The structural distance between the ground-truth and generated pockets, as proposed in Hayes et al. (2024). `TM-score`: The topological similarity between the generated and ground-truth pockets in local deviations. Aggregated Chai Score (`chai`): The confidence and structural validity of the pocket-substrate complex by running Chai (Chai, 2024). It is calculated as $0.2 \times pTM + 0.8 \times ipTM - 100 \times clash$, where pTM is the predicted template modeling score, $ipTM$ is the interface predicted template modeling score (as used in Jumper et al. (2021)), and the definition of `chai` is proposed by Chai (2024). Binding Affinity (`Kd`): The binding affinity between the generated catalytic pocket and the substrate conformation is computed using AutoDock Vina (Trott & Olson, 2010). Amino Acid Recovery (`AAR`): The overlap ratio between the predicted and ground-truth amino acid types in the generated pocket. Enzyme Commission Accuracy (`ECacc`): The accuracy of matching the EC-class of generated pockets with the ground-truth EC-class.

Table 2: Evaluation of structural validity of EnzymeFlow- and baseline-generated catalytic pockets. The binding affinities (`Kd`) and structural confidence (`chai`) are computed by performing docking on the catalytic pocket and substrate conformation using Vina (Trott & Olson, 2010) and Chai (Chai, 2024), respectively. We highlight top three results in **bold**, underline, and *italic*, respectively.

Model	`cRMSD` (↓)			`TM-score` (↑)			`Kd` (↓)	`chai` (↑)	`AAR` (↑)	`ECacc` (↑)
	Top1	Top10	Median	Top1	Top10	Median				
Eval Data		-			-		-4.65	-	-	-
DEPACT	9.25	9.75	11.16	0.238	0.206	0.149	-5.46	0.125	0.112	0.149
PocketGen	7.65	8.14	10.45	0.260	0.233	0.193	-5.01	0.121	0.176	0.152
RFDiffusionAA	9.13	9.77	11.92	0.269	0.245	0.198	**-12.71**	**0.232**	0.153	0.170
PocketFlow	7.42	8.09	10.01	0.268	*0.260*	0.197	-4.93	0.123	*0.207*	0.166
EnzymeFlow (T=50)	**6.94**	**7.57**	9.04	**0.290**	**0.262**	**0.209**	-5.03	0.129	**0.216**	**0.280**
w/o coevo	7.02	7.60	*9.15*	0.288	*0.260*	*0.205*	-4.86	0.123	0.196	0.246
w/o pretraining	*7.01*	*7.69*	9.29	*0.286*	0.261	0.207	-4.33	*0.134*	0.202	*0.255*
w/o coevo+pretraining	7.05	7.81	9.43	0.278	0.255	0.204	-4.72	0.125	0.154	0.221
EnzymeFlow (T=100)	6.97	**7.57**	**9.02**	0.283	0.258	0.207	*-5.31*	0.135	0.215	0.273

Results. We compare the structural validity between EnzymeFlow- and baseline-generated catalytic pockets in Tab. 2. EnzymeFlow and its ablation models outperform baseline models, including leading

[2]PocketFlow is not open-sourced yet, we implement and train it on EnzymeFill without fixing the backbones.

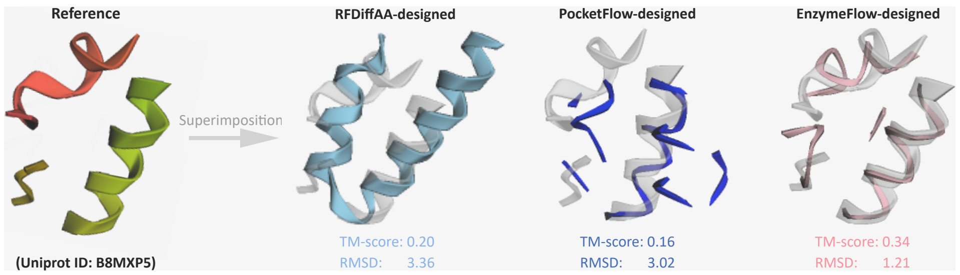

Figure 5: Case study of catalytic pocket design (UniProt: B8MXP5). We show the reference and designed pockets of different models. The pocket generation is conditioned on reaction `OC[C@H]1O[C@@H](Oc2ccccc2/C=C\\C(=O)O)[C@@H]([C@H]([C@@H]1O)O)O` → `OC(=O)/C=C\\c1ccccc1O` of EC3.

models like RFDiffusionAA and PocketFlow, with significant improvements in `cRMSD`, `TM-score`, and `ECacc`, and competitive performance in `AAR`. This demonstrates that EnzymeFlow is capable of generating more structurally valid catalytic pockets, aligning with the enzyme function analysis presented in Fig. 6. The average improvements over RFDiffusionAA in `cRMSD`, `TM-score`, `AAR`, and `EC-Acc` are 23.9%, 7.8%, 41.1%, and 64.7%, respectively. Additionally, EnzymeFlow slightly outperforms PocketFlow in catalytic-substrate binding, showing improved affinity scores (`Kd`) and structural confidence (`chai`) by 2.1% and 9.8%, respectively.

However, EnzymeFlow underperforms RFDiffusionAA in binding scores, reflected by lower affinities and structural confidence. However, considering that the affinities of EnzymeFlow-generated catalytic pockets (-5.03) are close to those of enzyme-reaction pairs in the evaluation set (-4.65), the binding of EnzymeFlow remains acceptable, as enzymes and substrates do not always require tight binding to catalyze reactions because of the kinetic mechanism (Cleland, 1977; Arcus & Mulholland, 2020).

5.2 Quantitative Analysis of Enzyme Function

The key question is how we can *quantitatively* assess enzyme functions, *i.e.,* catalytic ability, of the generated pockets for a given reaction. To answer this, we perform enzyme function analysis on the designed catalytic pockets. Accurate annotated enzyme function is important for catalytic pocket design because it helps identify the functionality and the active sites that should be preserved or modified to improve catalytic efficiency (Rost, 2002; Barglow & Cravatt, 2007; Yu et al., 2023).

Enzyme Function Comparison. In EnzymeFlow, we co-annotate the enzyme function alongside the catalytic pocket design, allowing their functions to directly influence the structure generation. This integration of enzyme function annotation into EnzymeFlow ensures functionality control throughout the design. For baselines that design general proteins rather than enzyme-specific pockets, we perform enzyme function annotation post-hoc using CLEAN (Yu et al., 2023) to classify and annotate the EC-class of the generated pockets. After labeling each generated pocket with a EC-class, we compare it to the ground-truth EC-class associated with the actual reaction to compute EC-class accuracy, which quantifies how well the generated pockets align with the intended enzyme functions.

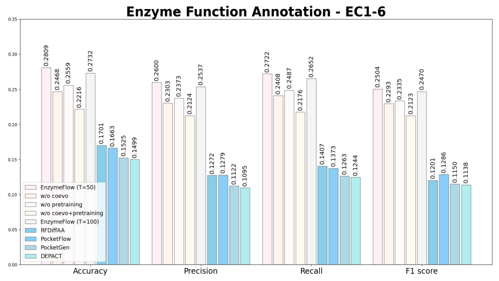

Figure 6: Quantitative comparison of annotated enzyme functions between EnzymeFlow- and baseline-generated catalytic pockets across all EC classes, using four multi-label accuracy metrics. Light color represents EnzymeFlow and its ablation models, blue color represents baseline pocket design models.

Results. We quantitatively compare the annotated enzyme functions between EnzymeFlow- and baseline-generated catalytic pockets across all EC classes in Fig. 6, and compare the per-class performance in Fig. 7. These figures allow us to interpret the functions of enzyme catalytic pockets designed by different models. From Fig. 6, EnzymeFlow and its ablation models achieve the highest values across various multi-label accuracy metrics, including accuracy (0.2809), precision (0.2600), recall (0.2722), and F1 score (0.2504), outperforming models like RFDiffusionAA and PocketFlow. Additionally, Fig. 7 illustrates per-class enzyme function accuracy, where EnzymeFlow demonstrates strong performance in EC2, EC4, EC5, and EC6, competitive performance in EC3, but slightly weaker performance in EC1 compared to baseline models. Baseline models tend to perform poorly in EC5 and EC6, with per-class occurrence and accuracy showing values close to 0. In contrast,

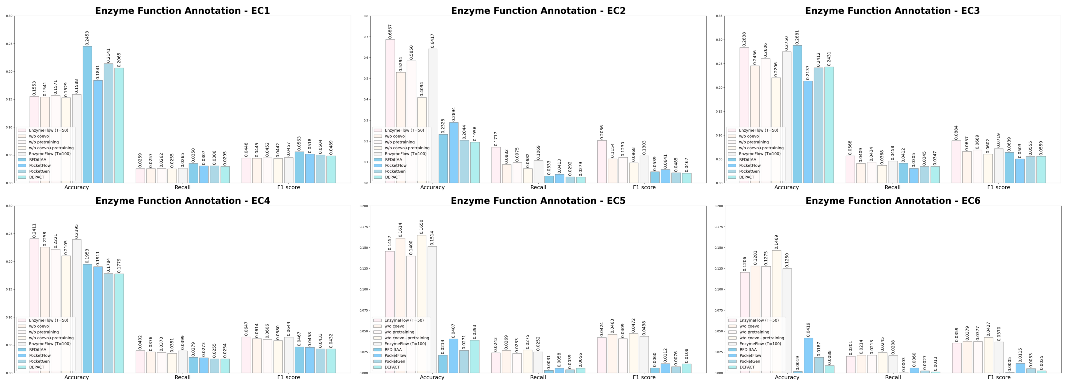
Figure 7: Quantitative comparison of annotated enzyme functions between EnzymeFlow- and baseline-generated catalytic pockets per EC-class, using accuracy, recall, and F1 score. Light color represents EnzymeFlow and ablation models, blue color represents baseline pocket design models.

EnzymeFlow generates more functionally diverse and accurate catalytic pockets, maintaining higher accuracy across different EC classes.

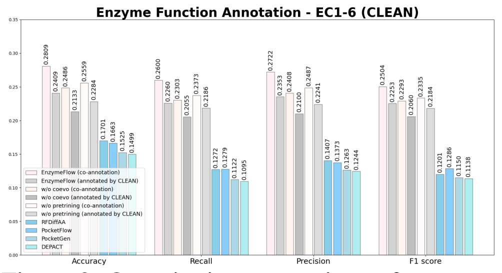
Figure 8: Quantitative comparison of annotated enzyme functions between EnzymeFlow- and baseline-generated catalytic pockets across all EC classes, using four multi-label accuracy metrics. Light color represents EnzymeFlow with enzyme function co-annotation, gray color represents EnzymeFlow with enzyme functions annotated by CLEAN post hoc, blue color represents baseline pocket design models with enzyme functions annotated by CLEAN post hoc.

Additionally, for a fairer comparison, in Fig. 8, we compare EnzymeFlow with co-generated enzyme functions, EnzymeFlow with functions annotated post hoc by CLEAN, and baseline models with functions also annotated post hoc by CLEAN. This comparison aims to evaluate the enzyme functions of generated catalytic pockets of different pocket design models using post-hoc function annotation via CLEAN. We observe that EnzymeFlow outperforms the baselines in multi-label accuracy metrics, even when functions are annotated post hoc.

In conclusion, EnzymeFlow generates catalytic pockets that are better compared to other pocket design models, providing more accurate and diverse enzyme functions, which suggests enhanced catalytic potential. From both functional and structural perspectives, the *function-based, reaction-conditioned* EnzymeFlow outperforms current *structure-based, substrate-conditioned* protein design models in both structural validity and intended function design (catalytic ability). EnzymeFlow leverages enzyme-reaction co-evolution to effectively capture the dynamic changes in catalytic reactions as substrates are transformed into products. This approach enables function-based enzyme design, resulting in the generation of more functionally and structurally valid catalytic pockets for specific reactions.

6 Limitation and Future Work

EnzymeFlow addresses key challenges in designing enzyme catalytic pockets for specific reactions, but several limitations remain. The first limitation is that EnzymeFlow currently generates only the catalytic pocket residues, rather than the entire enzyme structure. Ideally, the catalytic pocket should be designed first, followed by the design or reconstruction of the full enzyme structure based on the pocket. While we are developing to use ESM3 (Hayes et al., 2024) to reconstruct the full enzyme structure based on the designed catalytic pocket (discussed in App. I), this is not the most ideal solution. ESM3 is not specifically trained for enzyme-related tasks, which may limit its performance in enzyme design. In future versions of EnzymeFlow, we are working to fine-tune large biological models like ESM3 (Hayes et al., 2024), RFDiffusionAA (Krishna et al., 2024), or Genie2 (Lin et al., 2024) to specialize them for enzyme-related tasks, particularly for inpainting functional motifs of enzymes (enzyme catalytic motif scaffolding). Additionally, we aim to create an end-to-end model that combines EnzymeFlow with these large models, enabling catalytic pocket generation and functional motif inpainting in a single step, rather than in a two-step process. The second limitation, though minor, is that EnzymeFlow currently operates only on enzyme backbones and does not model or generate enzyme side chains. In future work, we plan to incorporate models like DiffPack (Zhang et al., 2024c) or develop a full-atom model to address this.

Reproducibility Statement

We provide our code and data examples with demonstrations at https://anonymous.4open.science/r/EnzymeFlow-7420. In particular, a Jupyter notebook demonstrating the *de novo* design of enzyme catalytic pockets conditioned on specific reactions is available at https://anonymous.4open.science/r/EnzymeFlow-7420/enzymeflow_demo.ipynb. For those who prefer not to dive into the full codebase, we have also open-sourced key model components in App. E, App. D, and other appendix sections.

References

Josh Abramson, Jonas Adler, Jack Dunger, Richard Evans, Tim Green, Alexander Pritzel, Olaf Ronneberger, Lindsay Willmore, Andrew J Ballard, Joshua Bambrick, et al. Accurate structure prediction of biomolecular interactions with alphafold 3. *Nature*, pp. 1–3, 2024.

Michael S. Albergo and Eric Vanden-Eijnden. Building normalizing flows with stochastic interpolants, 2023. URL https://arxiv.org/abs/2209.15571.

Mohammed AlQuraishi. End-to-end differentiable learning of protein structure. *Cell systems*, 8(4): 292–301, 2019.

Stephen F Altschul, Warren Gish, Webb Miller, Eugene W Myers, and David J Lipman. Basic local alignment search tool. *Journal of molecular biology*, 215(3):403–410, 1990.

Stephen F Altschul, Thomas L Madden, Alejandro A Schäffer, Jinghui Zhang, Zheng Zhang, Webb Miller, and David J Lipman. Gapped blast and psi-blast: a new generation of protein database search programs. *Nucleic acids research*, 25(17):3389–3402, 1997.

Vickery L Arcus and Adrian J Mulholland. Temperature, dynamics, and enzyme-catalyzed reaction rates. *Annual review of biophysics*, 49(1):163–180, 2020.

Minkyung Baek, Frank DiMaio, Ivan Anishchenko, Justas Dauparas, Sergey Ovchinnikov, Gyu Rie Lee, Jue Wang, Qian Cong, Lisa N Kinch, R Dustin Schaeffer, et al. Accurate prediction of protein structures and interactions using a three-track neural network. *Science*, 373(6557):871–876, 2021.

Amos Bairoch. The enzyme database in 2000. *Nucleic acids research*, 28(1):304–305, 2000.

Parit Bansal, Anne Morgat, Kristian B Axelsen, Venkatesh Muthukrishnan, Elisabeth Coudert, Lucila Aimo, Nevila Hyka-Nouspikel, Elisabeth Gasteiger, Arnaud Kerhornou, Teresa Batista Neto, et al. Rhea, the reaction knowledgebase in 2022. *Nucleic acids research*, 50(D1):D693–D700, 2022.

Katherine T Barglow and Benjamin F Cravatt. Activity-based protein profiling for the functional annotation of enzymes. *Nature methods*, 4(10):822–827, 2007.

Jesse D Bloom and Frances H Arnold. In the light of directed evolution: pathways of adaptive protein evolution. *Proceedings of the National Academy of Sciences*, 106(supplement_1):9995–10000, 2009.

Rosalin Bonetta and Gianluca Valentino. Machine learning techniques for protein function prediction. *Proteins: Structure, Function, and Bioinformatics*, 88(3):397–413, 2020.

Avishek Joey Bose, Tara Akhound-Sadegh, Kilian Fatras, Guillaume Huguet, Jarrid Rector-Brooks, Cheng-Hao Liu, Andrei Cristian Nica, Maksym Korablyov, Michael Bronstein, and Alexander Tong. Se (3)-stochastic flow matching for protein backbone generation. *arXiv preprint arXiv:2310.02391*, 2023.

Adam R Boyko, Scott H Williamson, Amit R Indap, Jeremiah D Degenhardt, Ryan D Hernandez, Kirk E Lohmueller, Mark D Adams, Steffen Schmidt, John J Sninsky, Shamil R Sunyaev, et al. Assessing the evolutionary impact of amino acid mutations in the human genome. *PLoS genetics*, 4(5):e1000083, 2008.

Andrew Campbell, Jason Yim, Regina Barzilay, Tom Rainforth, and Tommi Jaakkola. Generative flows on discrete state-spaces: Enabling multimodal flows with applications to protein co-design. *arXiv preprint arXiv:2402.04997*, 2024.

Eleanor Campbell, Miriam Kaltenbach, Galen J Correy, Paul D Carr, Benjamin T Porebski, Emma K Livingstone, Livnat Afriat-Jurnou, Ashley M Buckle, Martin Weik, Florian Hollfelder, et al. The role of protein dynamics in the evolution of new enzyme function. *Nature chemical biology*, 12 (11):944–950, 2016.

Ron Caspi, Richard Billington, Ingrid M Keseler, Anamika Kothari, Markus Krummenacker, Peter E Midford, Wai Kit Ong, Suzanne Paley, Pallavi Subhraveti, and Peter D Karp. The metacyc database of metabolic pathways and enzymes-a 2019 update. *Nucleic acids research*, 48(D1):D445–D453, 2020.

Chai. Chai-1 technical report. `https://chaiassets.com/chai-1/paper/technical_report_v1.pdf`, 2024.

Yaoxi Chen, Quan Chen, and Haiyan Liu. Depact and pacmatch: A workflow of designing de novo protein pockets to bind small molecules. *Journal of Chemical Information and Modeling*, 62(4): 971–985, 2022.

Alexander E Chu, Jinho Kim, Lucy Cheng, Gina El Nesr, Minkai Xu, Richard W Shuai, and Po-Ssu Huang. An all-atom protein generative model. *Proceedings of the National Academy of Sciences*, 121(27):e2311500121, 2024.

W Wallace Cleland. Determining the chemical mechanisms of enzyme-catalyzed reactions by kinetic studies. *Adv Enzymol Relat Areas Mol Biol*, 45:273–387, 1977.

Gene Ontology Consortium. The gene ontology (go) database and informatics resource. *Nucleic acids research*, 32(suppl_1):D258–D261, 2004.

Robert A Copeland. *Enzymes: a practical introduction to structure, mechanism, and data analysis*. John Wiley & Sons, 2023.

Gabriele Corso, Hannes Stärk, Bowen Jing, Regina Barzilay, and Tommi Jaakkola. Diffdock: Diffusion steps, twists, and turns for molecular docking. *arXiv preprint arXiv:2210.01776*, 2022.

Justas Dauparas, Gyu Rie Lee, Robert Pecoraro, Linna An, Ivan Anishchenko, Cameron Glasscock, and David Baker. Atomic context-conditioned protein sequence design using ligandmpnn. *Biorxiv*, pp. 2023–12, 2023.

Valerie de Crecy-Lagard, Raquel Dias, Iddo Friedberg, Yifeng Yuan, and Manal Swairjo. Limitations of current machine-learning models in predicting enzymatic functions for uncharacterized proteins. *bioRxiv*, pp. 2024–07, 2024.

Mark A DePristo, Daniel M Weinreich, and Daniel L Hartl. Missense meanderings in sequence space: a biophysical view of protein evolution. *Nature Reviews Genetics*, 6(9):678–687, 2005.

J-L Ferrer, MB Austin, C Stewart Jr, and JP Noel. Structure and function of enzymes involved in the biosynthesis of phenylpropanoids. *Plant Physiology and Biochemistry*, 46(3):356–370, 2008.

Hazel M Girvan and Andrew W Munro. Applications of microbial cytochrome p450 enzymes in biotechnology and synthetic biology. *Current opinion in chemical biology*, 31:136–145, 2016.

Margaret E Glasner, John A Gerlt, and Patricia C Babbitt. Evolution of enzyme superfamilies. *Current opinion in chemical biology*, 10(5):492–497, 2006.

Vladimir Gligorijević, P Douglas Renfrew, Tomasz Kosciolek, Julia Koehler Leman, Daniel Berenberg, Tommi Vatanen, Chris Chandler, Bryn C Taylor, Ian M Fisk, Hera Vlamakis, et al. Structure-based protein function prediction using graph convolutional networks. *Nature communications*, 12 (1):3168, 2021.

Tomas Hayes, Roshan Rao, Halil Akin, Nicholas J Sofroniew, Deniz Oktay, Zeming Lin, Robert Verkuil, Vincent Q Tran, Jonathan Deaton, Marius Wiggert, et al. Simulating 500 million years of evolution with a language model. *bioRxiv*, pp. 2024–07, 2024.

Esther Heid, Daniel Probst, William H Green, and Georg KH Madsen. Enzymemap: curation, validation and data-driven prediction of enzymatic reactions. *Chemical Science*, 14(48):14229–14242, 2023.

Maarten L Hekkelman, Ida de Vries, Robbie P Joosten, and Anastassis Perrakis. Alphafill: enriching alphafold models with ligands and cofactors. *Nature Methods*, 20(2):205–213, 2023.

C Eric Hodgman and Michael C Jewett. Cell-free synthetic biology: thinking outside the cell. *Metabolic engineering*, 14(3):261–269, 2012.

Chenqing Hua, Sitao Luan, Qian Zhang, and Jie Fu. Graph neural networks intersect probabilistic graphical models: A survey. *arXiv preprint arXiv:2206.06089*, 2022a.

Chenqing Hua, Guillaume Rabusseau, and Jian Tang. High-order pooling for graph neural networks with tensor decomposition. *Advances in Neural Information Processing Systems*, 35:6021–6033, 2022b.

Chenqing Hua, Sitao Luan, Minkai Xu, Rex Ying, Jie Fu, Stefano Ermon, and Doina Precup. Mudiff: Unified diffusion for complete molecule generation. *arXiv preprint arXiv:2304.14621*, 2023.

Chenqing Hua, Connor Coley, Guy Wolf, Doina Precup, and Shuangjia Zheng. Effective protein-protein interaction exploration with ppiretrieval. *arXiv preprint arXiv:2402.03675*, 2024a.

Chenqing Hua, Bozitao Zhong, Sitao Luan, Liang Hong, Guy Wolf, Doina Precup, and Shuangjia Zheng. Reactzyme: A benchmark for enzyme-reaction prediction. *arXiv preprint arXiv:2408.13659*, 2024b.

Jaime Huerta-Cepas, Damian Szklarczyk, Davide Heller, Ana Hernández-Plaza, Sofia K Forslund, Helen Cook, Daniel R Mende, Ivica Letunic, Thomas Rattei, Lars J Jensen, et al. eggnog 5.0: a hierarchical, functionally and phylogenetically annotated orthology resource based on 5090 organisms and 2502 viruses. *Nucleic acids research*, 47(D1):D309–D314, 2019.

Clemens Isert, Kenneth Atz, and Gisbert Schneider. Structure-based drug design with geometric deep learning. *Current Opinion in Structural Biology*, 79:102548, 2023.

Christian Jäckel, Peter Kast, and Donald Hilvert. Protein design by directed evolution. *Annu. Rev. Biophys.*, 37(1):153–173, 2008.

Roy A Jensen. Enzyme recruitment in evolution of new function. *Annual review of microbiology*, 30 (1):409–425, 1976.

John Jumper, Richard Evans, Alexander Pritzel, Tim Green, Michael Figurnov, Olaf Ronneberger, Kathryn Tunyasuvunakool, Russ Bates, Augustin Žídek, Anna Potapenko, et al. Highly accurate protein structure prediction with alphafold. *Nature*, 596(7873):583–589, 2021.

Jay D Keasling. Manufacturing molecules through metabolic engineering. *Science*, 330(6009): 1355–1358, 2010.

George A Khoury, James Smadbeck, Chris A Kieslich, and Christodoulos A Floudas. Protein folding and de novo protein design for biotechnological applications. *Trends in biotechnology*, 32(2): 99–109, 2014.

Joseph Kraut. How do enzymes work? *Science*, 242(4878):533–540, 1988.

Rohith Krishna, Jue Wang, Woody Ahern, Pascal Sturmfels, Preetham Venkatesh, Indrek Kalvet, Gyu Rie Lee, Felix S Morey-Burrows, Ivan Anishchenko, Ian R Humphreys, et al. Generalized biomolecular modeling and design with rosettafold all-atom. *Science*, 384(6693):eadl2528, 2024.

Alexander Kroll, Sahasra Ranjan, Martin KM Engqvist, and Martin J Lercher. A general model to predict small molecule substrates of enzymes based on machine and deep learning. *Nature communications*, 14(1):2787, 2023a.

Alexander Kroll, Yvan Rousset, Xiao-Pan Hu, Nina A Liebrand, and Martin J Lercher. Turnover number predictions for kinetically uncharacterized enzymes using machine and deep learning. *Nature Communications*, 14(1):4139, 2023b.

Maxat Kulmanov and Robert Hoehndorf. Deepgoplus: improved protein function prediction from sequence. *Bioinformatics*, 36(2):422–429, 2020.

Haitao Lin, Yufei Huang, Meng Liu, Xuanjing Li, Shuiwang Ji, and Stan Z Li. Diffbp: Generative diffusion of 3d molecules for target protein binding. *arXiv preprint arXiv:2211.11214*, 2022.

Yeqing Lin, Minji Lee, Zhao Zhang, and Mohammed AlQuraishi. Out of many, one: Designing and scaffolding proteins at the scale of the structural universe with genie 2. *arXiv preprint arXiv:2405.15489*, 2024.

Yaron Lipman, Ricky TQ Chen, Heli Ben-Hamu, Maximilian Nickel, and Matt Le. Flow matching for generative modeling. *arXiv preprint arXiv:2210.02747*, 2022.

Wenfang Liu and Ping Wang. Cofactor regeneration for sustainable enzymatic biosynthesis. *Biotechnology advances*, 25(4):369–384, 2007.

Xingchao Liu, Chengyue Gong, and Qiang Liu. Flow straight and fast: Learning to generate and transfer data with rectified flow, 2022. URL https://arxiv.org/abs/2209.03003.

Wei Lu, Jixian Zhang, Weifeng Huang, Ziqiao Zhang, Xiangyu Jia, Zhenyu Wang, Leilei Shi, Chengtao Li, Peter G Wolynes, and Shuangjia Zheng. Dynamicbind: Predicting ligand-specific protein-ligand complex structure with a deep equivariant generative model. *Nature Communications*, 15(1):1071, 2024.

Sitao Luan, Mingde Zhao, Chenqing Hua, Xiao-Wen Chang, and Doina Precup. Complete the missing half: Augmenting aggregation filtering with diversification for graph convolutional networks. *arXiv preprint arXiv:2008.08844*, 2020.

Sitao Luan, Chenqing Hua, Qincheng Lu, Jiaqi Zhu, Mingde Zhao, Shuyuan Zhang, Xiao-Wen Chang, and Doina Precup. Revisiting heterophily for graph neural networks. *Advances in neural information processing systems*, 35:1362–1375, 2022.

Sitao Luan, Chenqing Hua, Qincheng Lu, Liheng Ma, Lirong Wu, Xinyu Wang, Minkai Xu, Xiao-Wen Chang, Doina Precup, Rex Ying, et al. The heterophilic graph learning handbook: Benchmarks, models, theoretical analysis, applications and challenges. *arXiv preprint arXiv:2407.09618*, 2024a.

Sitao Luan, Chenqing Hua, Minkai Xu, Qincheng Lu, Jiaqi Zhu, Xiao-Wen Chang, Jie Fu, Jure Leskovec, and Doina Precup. When do graph neural networks help with node classification? investigating the homophily principle on node distinguishability. *Advances in Neural Information Processing Systems*, 36, 2024b.

Xizeng Mao, Tao Cai, John G Olyarchuk, and Liping Wei. Automated genome annotation and pathway identification using the kegg orthology (ko) as a controlled vocabulary. *Bioinformatics*, 21(19):3787–3793, 2005.

Andrew CR Martin, Christine A Orengo, E Gail Hutchinson, Susan Jones, Maria Karmirantzou, Roman A Laskowski, John BO Mitchell, Chiara Taroni, and Janet M Thornton. Protein folds and functions. *Structure*, 6(7):875–884, 1998.

Lukasz Maziarka, Tomasz Danel, Slawomir Mucha, Krzysztof Rataj, Jacek Tabor, and Stanislaw Jastrzebski. Molecule attention transformer. *arXiv preprint arXiv:2002.08264*, 2020.

Peter G Mikhael, Itamar Chinn, and Regina Barzilay. Clipzyme: Reaction-conditioned virtual screening of enzymes. *arXiv preprint arXiv:2402.06748*, 2024.

Yukito Murakami, Jun-ichi Kikuchi, Yoshio Hisaeda, and Osamu Hayashida. Artificial enzymes. *Chemical reviews*, 96(2):721–758, 1996.

Lianet Noda-Garcia, Wolfram Liebermeister, and Dan S Tawfik. Metabolite–enzyme coevolution: from single enzymes to metabolic pathways and networks. *Annual Review of Biochemistry*, 87(1): 187–216, 2018.

Noel M O'Boyle, Michael Banck, Craig A James, Chris Morley, Tim Vandermeersch, and Geoffrey R Hutchison. Open babel: An open chemical toolbox. *Journal of cheminformatics*, 3:1–14, 2011.

Csaba Pál, Balázs Papp, and Martin J Lercher. An integrated view of protein evolution. *Nature reviews genetics*, 7(5):337–348, 2006.

Marta Pelay-Gimeno, Adrian Glas, Oliver Koch, and Tom N Grossmann. Structure-based design of inhibitors of protein–protein interactions: mimicking peptide binding epitopes. *Angewandte Chemie International Edition*, 54(31):8896–8927, 2015.

Gaspar P Pinto, Marina Corbella, Andrey O Demkiv, and Shina Caroline Lynn Kamerlin. Exploiting enzyme evolution for computational protein design. *Trends in Biochemical Sciences*, 47(5): 375–389, 2022.

Roshan M Rao, Jason Liu, Robert Verkuil, Joshua Meier, John Canny, Pieter Abbeel, Tom Sercu, and Alexander Rives. Msa transformer. In *International Conference on Machine Learning*, pp. 8844–8856. PMLR, 2021.

Burkhard Rost. Enzyme function less conserved than anticipated. *Journal of molecular biology*, 318 (2):595–608, 2002.

Jae Yong Ryu, Hyun Uk Kim, and Sang Yup Lee. Deep learning enables high-quality and high-throughput prediction of enzyme commission numbers. *Proceedings of the National Academy of Sciences*, 116(28):13996–14001, 2019.

Vıctor Garcia Satorras, Emiel Hoogeboom, and Max Welling. E (n) equivariant graph neural networks. In *International conference on machine learning*, pp. 9323–9332. PMLR, 2021.

Ida Schomburg, Antje Chang, Oliver Hofmann, Christian Ebeling, Frank Ehrentreich, and Dietmar Schomburg. Brenda: a resource for enzyme data and metabolic information. *Trends in biochemical sciences*, 27(1):54–56, 2002.

Philippe Schwaller, Benjamin Hoover, Jean-Louis Reymond, Hendrik Strobelt, and Teodoro Laino. Extraction of organic chemistry grammar from unsupervised learning of chemical reactions. *Science Advances*, 7(15):eabe4166, 2021.

Tobias Sikosek and Hue Sun Chan. Biophysics of protein evolution and evolutionary protein biophysics. *Journal of The Royal Society Interface*, 11(100):20140419, 2014.

Hannes Stärk, Bowen Jing, Regina Barzilay, and Tommi Jaakkola. Harmonic self-conditioned flow matching for multi-ligand docking and binding site design. *arXiv preprint arXiv:2310.05764*, 2023.

Martin Steinegger and Johannes Söding. Mmseqs2 enables sensitive protein sequence searching for the analysis of massive data sets. *Nature biotechnology*, 35(11):1026–1028, 2017.

Janet M Thornton, Christine A Orengo, Annabel E Todd, and Frances MG Pearl. Protein folds, functions and evolution. *Journal of molecular biology*, 293(2):333–342, 1999.

Oleg Trott and Arthur J Olson. Autodock vina: improving the speed and accuracy of docking with a new scoring function, efficient optimization, and multithreading. *Journal of computational chemistry*, 31(2):455–461, 2010.

Jérôme Tubiana, Dina Schneidman-Duhovny, and Haim J Wolfson. Scannet: an interpretable geometric deep learning model for structure-based protein binding site prediction. *Nature Methods*, 19(6):730–739, 2022.

Bart van Beusekom, Wouter G Touw, Mahidhar Tatineni, Sandeep Somani, Gunaretnam Rajagopal, Jinquan Luo, Gary L Gilliland, Anastassis Perrakis, and Robbie P Joosten. Homology-based hydrogen bond information improves crystallographic structures in the pdb. *Protein Science*, 27 (3):798–808, 2018.

Michel van Kempen, Stephanie S Kim, Charlotte Tumescheit, Milot Mirdita, Cameron LM Gilchrist, Johannes Söding, and Martin Steinegger. Foldseek: fast and accurate protein structure search. *Biorxiv*, pp. 2022–02, 2022.

Jue Wang, Sidney Lisanza, David Juergens, Doug Tischer, Ivan Anishchenko, Minkyung Baek, Joseph L Watson, Jung Ho Chun, Lukas F Milles, Justas Dauparas, et al. Deep learning methods for designing proteins scaffolding functional sites. *BioRxiv*, pp. 2021–11, 2021.

Renxiao Wang, Xueliang Fang, Yipin Lu, and Shaomeng Wang. The pdbbind database: Collection of binding affinities for protein- ligand complexes with known three-dimensional structures. *Journal of medicinal chemistry*, 47(12):2977–2980, 2004.

Joseph L Watson, David Juergens, Nathaniel R Bennett, Brian L Trippe, Jason Yim, Helen E Eisenach, Woody Ahern, Andrew J Borst, Robert J Ragotte, Lukas F Milles, et al. De novo design of protein structure and function with rfdiffusion. *Nature*, 620(7976):1089–1100, 2023.

David Whitford. *Proteins: structure and function*. John Wiley & Sons, 2013.

Yu Xia and Michael Levitt. Simulating protein evolution in sequence and structure space. *Current Opinion in Structural Biology*, 14(2):202–207, 2004.

Zhaoping Xiong, Dingyan Wang, Xiaohong Liu, Feisheng Zhong, Xiaozhe Wan, Xutong Li, Zhaojun Li, Xiaomin Luo, Kaixian Chen, Hualiang Jiang, et al. Pushing the boundaries of molecular representation for drug discovery with the graph attention mechanism. *Journal of medicinal chemistry*, 63(16):8749–8760, 2019.

Jason Yang, Ariane Mora, Shengchao Liu, Bruce J Wittmann, Anima Anandkumar, Frances H Arnold, and Yisong Yue. Care: a benchmark suite for the classification and retrieval of enzymes. *arXiv preprint arXiv:2406.15669*, 2024.

Kevin K Yang, Zachary Wu, and Frances H Arnold. Machine-learning-guided directed evolution for protein engineering. *Nature methods*, 16(8):687–694, 2019.

Jason Yim, Andrew Campbell, Andrew YK Foong, Michael Gastegger, José Jiménez-Luna, Sarah Lewis, Victor Garcia Satorras, Bastiaan S Veeling, Regina Barzilay, Tommi Jaakkola, et al. Fast protein backbone generation with se (3) flow matching. *arXiv preprint arXiv:2310.05297*, 2023a.

Jason Yim, Brian L Trippe, Valentin De Bortoli, Emile Mathieu, Arnaud Doucet, Regina Barzilay, and Tommi Jaakkola. Se (3) diffusion model with application to protein backbone generation. *arXiv preprint arXiv:2302.02277*, 2023b.

Tianhao Yu, Haiyang Cui, Jianan Canal Li, Yunan Luo, Guangde Jiang, and Huimin Zhao. Enzyme function prediction using contrastive learning. *Science*, 379(6639):1358–1363, 2023.

Odin Zhang, Yufei Huang, Shichen Cheng, Mengyao Yu, Xujun Zhang, Haitao Lin, Yundian Zeng, Mingyang Wang, Zhenxing Wu, Huifeng Zhao, et al. Deep geometry handling and fragment-wise molecular 3d graph generation. *arXiv preprint arXiv:2404.00014*, 2024a.

Odin Zhang, Jieyu Jin, Haitao Lin, Jintu Zhang, Chenqing Hua, Yufei Huang, Huifeng Zhao, Chang-Yu Hsieh, and Tingjun Hou. Ecloudgen: Access to broader chemical space for structure-based molecule generation. *bioRxiv*, pp. 2024–06, 2024b.

Xujun Zhang, Odin Zhang, Chao Shen, Wanglin Qu, Shicheng Chen, Hanqun Cao, Yu Kang, Zhe Wang, Ercheng Wang, Jintu Zhang, et al. Efficient and accurate large library ligand docking with karmadock. *Nature Computational Science*, 3(9):789–804, 2023a.

Yangtian Zhang, Zuobai Zhang, Bozitao Zhong, Sanchit Misra, and Jian Tang. Diffpack: A torsional diffusion model for autoregressive protein side-chain packing. *Advances in Neural Information Processing Systems*, 36, 2024c.

Zaixi Zhang, Zepu Lu, Hao Zhongkai, Marinka Zitnik, and Qi Liu. Full-atom protein pocket design via iterative refinement. *Advances in Neural Information Processing Systems*, 36:16816–16836, 2023b.

Zaixi Zhang, Wanxiang Shen, Qi Liu, and Marinka Zitnik. Pocketgen: Generating full-atom ligand-binding protein pockets. *bioRxiv*, pp. 2024–02, 2024d.

Zaixi Zhang, Marinka Zitnik, and Qi Liu. Generalized protein pocket generation with prior-informed flow matching, 2024e. URL https://arxiv.org/abs/2409.19520.

Zuobai Zhang, Minghao Xu, Arian Jamasb, Vijil Chenthamarakshan, Aurelie Lozano, Payel Das, and Jian Tang. Protein representation learning by geometric structure pretraining. *arXiv preprint arXiv:2203.06125*, 2022.

Emile Zuckerkandl and Linus Pauling. Molecules as documents of evolutionary history. *Journal of theoretical biology*, 8(2):357–366, 1965.

A Future Work in Progress: AI-driven Enzyme Design Platform

As discussed in Sec. 6, there are several limitations in the current version of EnzymeFlow. Here, we briefly outline the next steps and improvements we are actively working on for the upcoming version. Currently, EnzymeFlow generates only catalytic pocket residues rather than full enzyme structures. Ideally, the catalytic pocket should be designed first, followed by the reconstruction of the full enzyme structure based on the pocket. While we currently use ESM3 (Hayes et al., 2024) for this reconstruction, this approach is not ideal. Fine-tuning ESM3 or RFDiffusionAA (Krishna et al., 2024) would be preferable, but unfortunately, training scripts for these wonderful models are not provided, making it impossible to directly fine-tune them on our EnzymeFill dataset.

To address this, we are borrowing concepts from Wang et al. (2021) and Lin et al. (2024), which focuses on inpainting proteins and scaffolding functional motifs. We are working to integrate this concept into EnzymeFlow's pipeline, as part of our primary design. Our goal is to develop an end-to-end automated AI-driven enzyme discovery system that works as follows:

- 1. **Catalytic Pocket Design**: The system will first design enzyme catalytic pockets.
- 2. **Scaffolding Functional Motifs**: Next, it will scaffold the functional motifs to generate full enzyme structures.
- 3. **Substrate Docking**: Using methods like DiffDock (Corso et al., 2022), DynamicBind (Lu et al., 2024), or fine-tuned Chai (Chai, 2024) on EnzymeFill, the system will bind substrates to the catalytic pockets.
- 4. **Inverse Folding**: The enzyme-substrate complex will undergo inverse folding using LigandMPNN (Dauparas et al., 2023).
- 5. **Computational Screening**: Finally, the system will perform computational screening to select the best-generated enzymes.

This entire process is being developed into an integrated, end-to-end solution for AI-driven enzyme design. We are very excited about the potential of this project and look forward to achieving a fully automated enzyme design system in the near future.

B Open Discussion: Why is Substrate/Reaction-specified Enzyme Design Needed?

EnzymeFlow is unique in its leading approach to function-based *de novo* protein design. Currently, most protein design models, whether focused on backbone generation (Yim et al., 2023a;b; Bose et al., 2023; Campbell et al., 2024; Krishna et al., 2024) or pocket design (Zhang et al., 2023b;a; 2024d;e), are structure-based. These models aim to design or modify proteins to achieve a specific 3D structure, prioritizing stability, folding, and molecular interactions. The design process typically involves optimizing a protein structure to minimize energy and achieve a stable structural conformation (Khoury et al., 2014; Pelay-Gimeno et al., 2015).

In contrast, function-based protein design focuses on creating proteins that perform specific biochemical tasks, such as catalysis, signaling, or even binding (Martin et al., 1998; Thornton et al., 1999). These models are driven by the need for proteins to carry out particular functions rather than adopt a specific 3D structure. Function-based design often targets the active site or binding pockets, optimizing them for specific molecular interactions—in our case, the enzyme's catalytic pockets.

Our philosophy is that protein function determines its structure, meaning that a protein folds into a specific 3D shape to achieve its intended function, and the resulting structure can then be translated into a proper sequence—essentially, *protein function* $\rightarrow$ *protein structure* $\rightarrow$ *protein sequence*. EnzymeFlow follows this philosophy. Specifically, the function of an enzyme is determined by its ability to catalyze a specific reaction or interact with a specific substrate. Therefore, our enzyme pocket design process begins with the reaction or substrate in mind, incorporating reaction/substrate specificity into the generation process. The reaction or substrate represents the functional target for the generated enzyme pockets.

In this approach, EnzymeFlow generates enzyme pocket structures specified for the desired protein function, which contrasts with current generative methods that prioritize structure first. These existing methods operate on the idea that *protein structure* $\rightarrow$ *protein function* $\rightarrow$ *protein sequence*. However, proteins should be designed primarily for their functionality, not just their structures. EnzymeFlow's focus on function-based design could serve as an inspiration for future advancements, leading the way toward more purposeful, function-driven protein design.

C Related Work

C.1 Protein Representation Learning

Graph representation learning emerges as a potent strategy for representing and learning about proteins and molecules, focusing on structured, non-Euclidean data (Satorras et al., 2021; Luan et al., 2020; 2022; Hua et al., 2022a;b; Luan et al., 2024b;a). In this context, proteins and molecules can be effectively modeled as 2D graphs or 3D point clouds, where nodes correspond to individual atoms or residues, and edges represent interactions between them (Gligorijević et al., 2021; Zhang et al., 2022; Hua et al., 2023; Zhang et al., 2024a). Indeed, representing proteins and molecules as graphs or point clouds offers a valuable approach for gaining insights into and learning the fundamental geometric and chemical mechanisms governing protein-ligand interactions. This representation allows for a more comprehensive exploration of the intricate relationships and structural features within protein-ligand structures (Tubiana et al., 2022; Isert et al., 2023; Zhang et al., 2024b).

C.2 Protein Function Annotation

Protein function prediction aims to determine the biological role of a protein based on its sequence, structure, or other features. It is a crucial task in bioinformatics, often leveraging databases such as Gene Ontology (GO), Enzyme Commission (EC) numbers, and KEGG Orthology (KO) annotations (Bairoch, 2000; Consortium, 2004; Mao et al., 2005). Traditional methods like BLAST, PSI-BLAST, and eggNOG infer function by comparing sequence alignments and similarities (Altschul et al., 1990; 1997; Huerta-Cepas et al., 2019). Recently, deep learning has introduced more advanced approaches for protein function prediction (Ryu et al., 2019; Kulmanov & Hoehndorf, 2020; Bonetta & Valentino, 2020). There are two major types of function prediction models, one uses only protein sequence as their input, while the other also uses experimentally-determined or predicted protein structure as input. Typically, these methods predict EC or GO annotations to approximate protein functions, rather than describing the exact catalyzed reaction, which is a limitation of these approaches.

C.3 Protein Evolution

Protein evolution learns how proteins change over time through processes such as mutation, selection, and genetic drift (Pál et al., 2006; Bloom & Arnold, 2009), which influence protein functions. Studies on protein evolution focus on understanding the molecular mechanisms driving changes in protein sequences and structures. Zuckerkandl & Pauling (1965) introduce the concept of the molecular clock, which postulates that proteins evolve at a relatively constant rate over time, providing a framework for estimating divergence times between species. DePristo et al. (2005) show that evolutionary rates are influenced by functional constraints, with regions critical to protein function (*e.g.*, active sites, binding interfaces) evolving more slowly due to purifying selection. This understanding leads to the development of methods for detecting functionally important residues based on evolutionary conservation. Understanding protein evolution has practical applications in protein engineering. By studying how natural proteins evolve to acquire new functions, researchers design synthetic proteins with desired properties (Xia & Levitt, 2004; Jäckel et al., 2008). Additionally, deep learning models increasingly integrate evolutionary principles to predict protein function and stability, design novel enzymes, and guide protein engineering (Yang et al., 2019; AlQuraishi, 2019; Jumper et al., 2021).

C.4 Generative Models for Protein and Pocket Design

Recent advancements in generative models have advanced the field of protein design and binding pocket design, enabling the creation of proteins or binding pockets with desired properties and functions (Yim et al., 2023a;b; Chu et al., 2024; Hua et al., 2024a; Abramson et al., 2024). For example, RFDiff (Watson et al., 2023) employs denoising diffusion in conjunction with RoseTTAFold (Baek et al., 2021) for *de novo* protein structure design, achieving wet-lab-level generated structures that can be extended to binding pocket design. RFDiffusionAA (Krishna et al., 2024) extends RFDiff for joint modeling of protein and ligand structures, generating ligand-binding proteins and further leveraging GNNs for sequence design. Additionally, FAIR (Zhang et al., 2023b) and PocketGen

(Zhang et al., 2024d) use a two-stage coarse-to-fine refinement approach to co-design pocket structures and sequences. Recent models leveraging flow matching frameworks have shown promising results in these tasks. For instance, FoldFlow (Bose et al., 2023) introduces a series of flow models for protein backbone design, improving training stability and efficiency. FrameFlow (Yim et al., 2023a) further enhances sampling efficiency and demonstrates success in motif-scaffolding tasks using flow matching, while MultiFlow (Campbell et al., 2024) advances to structure and sequence co-design. These flow models, initially applied to protein backbones, have been further generalized to binding pockets. For example, PocketFlow (Zhang et al., 2024e) combines flow matching with physical priors to explicitly learn protein-ligand interaction types in pocket design, achieving superior results compared to RFDiffusionAA. While these models excel in protein and binding pocket design, they primarily focus on static protein(-ligand) interactions and lack the ability to model the chemical transformations involved in enzyme-substrate interactions. This limitation may reduce their accuracy and generalizability in designing enzyme pockets for catalytic reactions.

D Co-Evolutionary MSA Transformer

Co-evolution captures the dynamic relationship between an enzyme and its substrate during a catalytic reaction. AlphaFold2 (Jumper et al., 2021) has demonstrated the critical importance of leveraging protein evolution, specifically through multiple sequence alignments (MSA) across protein sequences, to enhance a model's generalizability and expressive power. Previous works, such as MSA Transformer (Rao et al., 2021) and EvoFormer (Jumper et al., 2021), have focused on encoding and learning protein evolution from MSA results. Proper co-evolution encodings of enzymes and reactions are essential for capturing the dynamic changes that occur during catalytic processes, not only in our EnzymeFlow model but in other models as well.

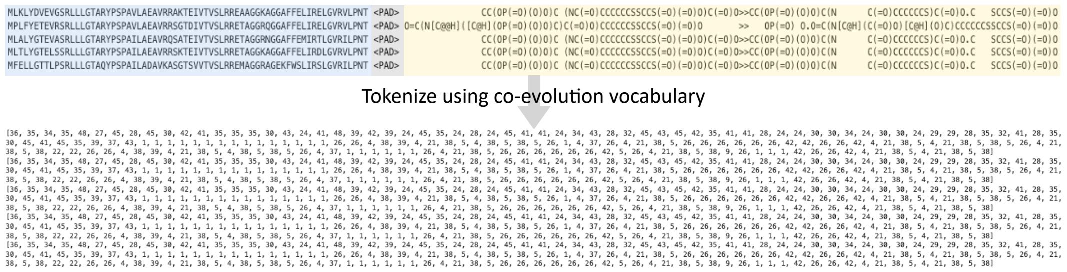
```
MLKLYDVEVGSRLLLGTARYPSPAVLAEAVRRAKTEIVTVSLRREAAGGKAGGAFFELIRELGVRVLPNT <PAD>             CC(OP(=O)(O)O)C (NC(=O)CCCCCCSSCCS(=O)(=O)O)C(=O)O>>CC(OP(=O)(O)O)C(N      C(=O)CCCCCCS)C(=O)O.C   SCCS(=O)(=O)O
MPLFYETEVRSRLLLGTARYPSPAVLAEAVRRSGTDIVTVSLRRETAGGRQGGAFFELIRELGVRVLPNT <PAD> O=C(N[C@@H]([C@H](OP(=O)(O)O)C)C(=O)O)CCCCCCSSCCS(=O)(=O)O      >>   OP(=O) O.O=C(N[C@H](C(=O)O)[C@H](O)C)CCCCCCSSCCS(=O)(=O)O
MLALYGTEVASRLLLGTARYPSPAILAEAVRQSATEIVTVSLRRETAGGRNGGAFFEMIRTLGVRILPNT <PAD>             CC(OP(=O)(O)O)C (NC(=O)CCCCCCSSCCS(=O)(=O)O)C(=O)O>>CC(OP(=O)(O)O)C(N      C(=O)CCCCCCS)C(=O)O.C   SCCS(=O)(=O)O
MLTLYGTELSSRLLLGTARYPSPAILAEAVRRSKTEIVTVSLRRETAGGKAGGAFFELIRDLGVRVLPNT <PAD>             CC(OP(=O)(O)O)C (NC(=O)CCCCCCSSCCS(=O)(=O)O)C(=O)O>>CC(OP(=O)(O)O)C(N      C(=O)CCCCCCS)C(=O)O.C   SCCS(=O)(=O)O
MFELLGTTLPSRLLLGTAQYPSPAILADAVKASGTSVVTVSLRREMAGGRAGEKFWSLIRSLGVRILPNT <PAD>             CC(OP(=O)(O)O)C (NC(=O)CCCCCCSSCCS(=O)(=O)O)C(=O)O>>CC(OP(=O)(O)O)C(N      C(=O)CCCCCCS)C(=O)O.C   SCCS(=O)(=O)O
```

```
[36, 35, 34, 35, 48, 27, 45, 28, 45, 30, 42, 41, 35, 35, 35, 30, 43, 24, 41, 48, 39, 42, 39, 24, 45, 35, 24, 28, 24, 45, 41, 41, 24, 34, 43, 28, 32, 45, 43, 45, 42, 35, 41, 41, 28, 24, 24, 30, 30, 34, 24, 30, 30, 24, 29, 29, 28, 35, 32, 41, 28, 35,
30, 45, 41, 45, 35, 39, 37, 43, 1, 1, 1, 1, 1, 1, 1, 1, 1, 1, 1, 1, 1, 1, 1, 26, 26, 4, 38, 39, 4, 21, 38, 5, 4, 38, 5, 38, 5, 26, 1, 4, 37, 26, 4, 21, 38, 5, 26, 26, 26, 26, 26, 26, 42, 42, 26, 26, 42, 4, 21, 38, 5, 4, 21, 38, 5, 38, 5, 26, 4, 21,
38, 5, 38, 22, 22, 26, 26, 4, 38, 39, 4, 21, 38, 5, 4, 38, 5, 38, 5, 26, 4, 37, 1, 1, 1, 1, 1, 1, 26, 4, 21, 38, 5, 26, 26, 26, 26, 26, 26, 42, 5, 26, 4, 21, 38, 5, 38, 9, 26, 1, 1, 1, 42, 26, 26, 42, 4, 21, 38, 5, 4, 21, 38, 5, 38]
[36, 35, 34, 35, 48, 27, 45, 28, 45, 30, 42, 41, 35, 35, 35, 30, 43, 24, 41, 48, 39, 42, 39, 24, 45, 35, 24, 28, 24, 45, 41, 41, 24, 34, 43, 28, 32, 45, 43, 45, 42, 35, 41, 41, 28, 24, 24, 30, 30, 34, 24, 30, 30, 24, 29, 29, 28, 35, 32, 41, 28, 35,
30, 45, 41, 45, 35, 39, 37, 43, 1, 1, 1, 1, 1, 1, 1, 1, 1, 1, 1, 1, 1, 1, 1, 26, 26, 4, 38, 39, 4, 21, 38, 5, 4, 38, 5, 38, 5, 26, 1, 4, 37, 26, 4, 21, 38, 5, 26, 26, 26, 26, 26, 26, 42, 42, 26, 26, 42, 4, 21, 38, 5, 4, 21, 38, 5, 38, 5, 26, 4, 21,
38, 5, 38, 22, 22, 26, 26, 4, 38, 39, 4, 21, 38, 5, 4, 38, 5, 38, 5, 26, 4, 37, 1, 1, 1, 1, 1, 1, 26, 4, 21, 38, 5, 26, 26, 26, 26, 26, 26, 42, 5, 26, 4, 21, 38, 5, 38, 9, 26, 1, 1, 1, 42, 26, 26, 42, 4, 21, 38, 5, 4, 21, 38, 5, 38]
[36, 35, 34, 35, 48, 27, 45, 28, 45, 30, 42, 41, 35, 35, 35, 30, 43, 24, 41, 48, 39, 42, 39, 24, 45, 35, 24, 28, 24, 45, 41, 41, 24, 34, 43, 28, 32, 45, 43, 45, 42, 35, 41, 41, 28, 24, 24, 30, 30, 34, 24, 30, 30, 24, 29, 29, 28, 35, 32, 41, 28, 35,
30, 45, 41, 45, 35, 39, 37, 43, 1, 1, 1, 1, 1, 1, 1, 1, 1, 1, 1, 1, 1, 1, 1, 26, 26, 4, 38, 39, 4, 21, 38, 5, 4, 38, 5, 38, 5, 26, 1, 4, 37, 26, 4, 21, 38, 5, 26, 26, 26, 26, 26, 26, 42, 42, 26, 26, 42, 4, 21, 38, 5, 4, 21, 38, 5, 38, 5, 26, 4, 21,
38, 5, 38, 22, 22, 26, 26, 4, 38, 39, 4, 21, 38, 5, 4, 38, 5, 38, 5, 26, 4, 37, 1, 1, 1, 1, 1, 1, 26, 4, 21, 38, 5, 26, 26, 26, 26, 26, 26, 42, 5, 26, 4, 21, 38, 5, 38, 9, 26, 1, 1, 1, 42, 26, 26, 42, 4, 21, 38, 5, 4, 21, 38, 5, 38]
[36, 35, 34, 35, 48, 27, 45, 28, 45, 30, 42, 41, 35, 35, 35, 30, 43, 24, 41, 48, 39, 42, 39, 24, 45, 35, 24, 28, 24, 45, 41, 41, 24, 34, 43, 28, 32, 45, 43, 45, 42, 35, 41, 41, 28, 24, 24, 30, 30, 34, 24, 30, 30, 24, 29, 29, 28, 35, 32, 41, 28, 35,
30, 45, 41, 45, 35, 39, 37, 43, 1, 1, 1, 1, 1, 1, 1, 1, 1, 1, 1, 1, 1, 1, 1, 26, 26, 4, 38, 39, 4, 21, 38, 5, 4, 38, 5, 38, 5, 26, 1, 4, 37, 26, 4, 21, 38, 5, 26, 26, 26, 26, 26, 26, 42, 42, 26, 26, 42, 4, 21, 38, 5, 4, 21, 38, 5, 38, 5, 26, 4, 21,
38, 5, 38, 22, 22, 26, 26, 4, 38, 39, 4, 21, 38, 5, 4, 38, 5, 38, 5, 26, 4, 37, 1, 1, 1, 1, 1, 1, 26, 4, 21, 38, 5, 26, 26, 26, 26, 26, 26, 42, 5, 26, 4, 21, 38, 5, 38, 9, 26, 1, 1, 1, 42, 26, 26, 42, 4, 21, 38, 5, 4, 21, 38, 5, 38]
[36, 35, 34, 35, 48, 27, 45, 28, 45, 30, 42, 41, 35, 35, 35, 30, 43, 24, 41, 48, 39, 42, 39, 24, 45, 35, 24, 28, 24, 45, 41, 41, 24, 34, 43, 28, 32, 45, 43, 45, 42, 35, 41, 41, 28, 24, 24, 30, 30, 34, 24, 30, 30, 24, 29, 29, 28, 35, 32, 41, 28, 35,
30, 45, 41, 45, 35, 39, 37, 43, 1, 1, 1, 1, 1, 1, 1, 1, 1, 1, 1, 1, 1, 1, 1, 26, 26, 4, 38, 39, 4, 21, 38, 5, 4, 38, 5, 38, 5, 26, 1, 4, 37, 26, 4, 21, 38, 5, 26, 26, 26, 26, 26, 26, 42, 42, 26, 26, 42, 4, 21, 38, 5, 4, 21, 38, 5, 38, 5, 26, 4, 21,
38, 5, 38, 22, 22, 26, 26, 4, 38, 39, 4, 21, 38, 5, 4, 38, 5, 38, 5, 26, 4, 37, 1, 1, 1, 1, 1, 1, 26, 4, 21, 38, 5, 26, 26, 26, 26, 26, 26, 42, 5, 26, 4, 21, 38, 5, 38, 9, 26, 1, 1, 1, 42, 26, 26, 42, 4, 21, 38, 5, 4, 21, 38, 5, 38]
```

Figure 9: Enzyme-reaction co-evolution and tokenized representation.

D.1 Co-evolution vocabulary

We provide our co-evolution dictionary for tokenization and encoding following:

```
{'<pad>': 0, ' ': 1, '#': 2, '%': 3, '(': 4, ')': 5, '*': 6, '+': 7, '-': 8, '.': 9,
'/': 10, '0': 11, '1': 12, '2': 13, '3': 14, '4': 15, '5': 16, '6': 17, '7': 18,
'8': 19, '9': 20, '=': 21, '>': 22, '@': 23, 'A': 24, 'B': 25, 'C': 26, 'D': 27,
'E': 28, 'F': 29, 'G': 30, 'H': 31, 'I': 32, 'J': 33, 'K': 34, 'L': 35, 'M': 36,
'N': 37, 'O': 38, 'P': 39, 'Q': 40, 'R': 41, 'S': 42, 'T': 43, 'U': 44, 'V': 45,
'W': 46, 'X': 47, 'Y': 48, 'Z': 49, '[': 50, '\\': 51, ']': 52, 'c': 53, 'e': 54,
'g': 55, 'i': 56, 'l': 57, 'n': 58, 'o': 59, 'r': 60, 's': 61, 'u': 62, '<unk>': 63}
```

Figure 10: EnzymeFlow co-evolution dictionary.

D.2 coEvoFormer Implementation

Here, we introduce a new co-evolutionary MSA transformer, coEvoFormer. The co-evolution of an enzyme-reaction pair is represented by a matrix $U \in \mathbb{R}^{N_{\text{MSA}} \times N_{\text{token}}}$, which combines the MSA results of enzyme sequences and reaction SMILES (illustrated in Fig. 3(3d)). In this matrix, N_{MSA} denotes the number of MSA sequences, and N_{token} denotes the length of the preserved MSA alignment. Each element $u^{mn} \in \{1, \ldots, 64\} \cup \{\times\}$ in U represents a tokenized character from our co-evolution vocabulary (provided in App. D.1), with $\times$ indicating the *masking state*. The coEvoFormer takes the co-evolution matrix U as input and outputs an embedded co-evolution representation $H_U \in \mathbb{R}^{N_{\text{MSA}} \times N_{\text{token}} \times D_{H_U}}$, where D_{H_U} denotes the hidden dimension size.

The code for coEvoFormer follows directly:

```python
import math, copy
import numpy as np

import torch
import torch.nn as nn
import torch.nn.functional as F
from torch.autograd import Variable

## Co-Evolution Transformer (coEvoFormer)

## (12) Layer Norm
class ResidualNorm(nn.Module):
    def __init__(self, size, dropout):
        super(ResidualNorm, self).__init__()
        self.norm = LayerNorm(size)
        self.dropout = nn.Dropout(dropout)

    def forward (self, x, sublayer):
        return x + self.dropout(sublayer(self.norm(x)))


## (11) Residual Norm
class LayerNorm(nn.Module):
    def __init__(self, features, eps=1e-6):
        super(LayerNorm, self).__init__()
        self.a_2 = nn.Parameter(torch.ones(features))
        self.b_2 = nn.Parameter(torch.zeros(features))
        self.eps = eps

    def forward(self, x):
        mean = x.mean(-1, keepdim=True)
        std = x.std(-1, keepdim=True)
        x = self.a_2 * (x - mean) / (std + self.eps) + self.b_2
        return x


## (10) 2-layer MLP
class MLP(nn.Module):
    def __init__(self, model_depth, ff_depth, dropout):
        super(MLP, self).__init__()
        self.w1 = nn.Linear(model_depth, ff_depth)
        self.w2 = nn.Linear(ff_depth, model_depth)
        self.dropout = nn.Dropout(dropout)
        self.silu = nn.SiLU()

    def forward(self, x):
        return self.w2(self.dropout(self.silu(self.w1(x))))


## (9) Attention
def attention(Q,K,V, mask=None):
    dk = Q.size(-1)
    T = (Q @ K.transpose(-2, -1))/math.sqrt(dk)
    if mask is not None:
        T = T.masked_fill_(mask.unsqueeze(1)==0, -1e9)
    T = F.softmax(T, dim=-1)
    return T @ V


## (8) Multi-Head Attention
class MultiHeadAttention(nn.Module):
    def __init__ (self,
                  num_heads,
                  embed_dim,
                  bias=False
                 ):
        super(MultiHeadAttention, self).__init__()
        self.num_heads = num_heads
        self.dk = embed_dim//num_heads
        self.WQ = nn.Linear(embed_dim, embed_dim, bias=bias)
        self.WK = nn.Linear(embed_dim, embed_dim, bias=bias)
        self.WV = nn.Linear(embed_dim, embed_dim, bias=bias)
        self.WO = nn.Linear(embed_dim, embed_dim, bias=bias)

    def forward(self, x, kv, mask=None):
        batch_size = x.size(0)
        Q = self.WQ(x ).view(batch_size, -1, self.num_heads, self.dk).transpose(1,2)
        K = self.WK(kv).view(batch_size, -1, self.num_heads, self.dk).transpose(1,2)
        V = self.WV(kv).view(batch_size, -1, self.num_heads, self.dk).transpose(1,2)
        if mask is not None:
            if len(mask.shape) == 2:
                mask = torch.einsum('bi,bj->bij', mask, mask)
        x = attention(Q, K, V, mask=mask)

        x = x.transpose(1, 2).contiguous().view(batch_size, -1, self.num_heads*self.dk)
        return self.WO(x)


## (7) Positional Embedding
class PositionalEncoding(nn.Module):
    def __init__(self, model_depth, max_len=5000):
        super(PositionalEncoding, self).__init__()

        pe = torch.zeros(max_len, model_depth)
        position = torch.arange(0.0, max_len).unsqueeze(1)
        div_term = torch.exp(torch.arange(0.0, model_depth, 2) *
                             -(math.log(10000.0) / model_depth))
        pe[:, 0::2] = torch.sin(position * div_term)
        pe[:, 1::2] = torch.cos(position * div_term)
        pe = pe.unsqueeze(0)
        self.register_buffer('pe', pe)

    def forward(self, x):
        return x + Variable(self.pe[:, :x.size(1)], requires_grad=False)


## (6) Embedding
class Embedding(nn.Module):
    def __init__(self, vocab_size, model_depth):
        super(Embedding, self).__init__()
        self.lut = nn.Embedding(vocab_size, model_depth)
        self.model_depth = model_depth
        self.positional = PositionalEncoding(model_depth)

    def forward(self, x):
        emb = self.lut(x) * math.sqrt(self.model_depth)
        return self.positional(emb)


## (5) Encoder Layer
class EncoderLayer(nn.Module):
    def __init__(self,
                  n_heads,
                  model_depth,
                  ff_depth,
                  dropout=0.0
                 ):
        super(EncoderLayer, self).__init__()
        self.self_attn = MultiHeadAttention(embed_dim=model_depth, num_heads=n_heads)
        self.resnorm1 = ResidualNorm(model_depth, dropout)
        self.ff = MLP(model_depth, ff_depth, dropout)
        self.resnorm2 = ResidualNorm(model_depth, dropout)

    def forward(self, x, mask):
        x = self.resnorm1(x, lambda arg: self.self_attn(arg, arg, mask))
        x = self.resnorm2(x, self.ff)
        return x


## (4) Encoder
class Encoder(nn.Module):
    def __init__ (self,
                  n_layers,
                  n_heads,
                  model_depth,
                  ff_depth,
                  dropout
                 ):
        super(Encoder, self).__init__()
        self.layers = nn.ModuleList([EncoderLayer(n_heads, model_depth, ff_depth, dropout) for
      i in range(n_layers)])
        self.lnorm = LayerNorm(model_depth)

    def forward(self, x, mask):
        for layer in self.layers:
            x = layer(x, mask)
        return self.lnorm(x)
```

```
## (3)Generator
class Generator(nn.Module):
    def __init__(self,
                 model_depth,
                 vocab_size
                ):
        super(Generator, self).__init__()
        self.ff = nn.Linear(model_depth, vocab_size)

    def forward(self, x):
        return F.log_softmax(self.ff(x), dim=-1)


## (2)coEvoEmbedder
class CoEvoEmbedder(nn.Module):
    def __init__(self,
                 vocab_size,
                 n_layers=2,
                 n_heads=4,
                 model_depth=64,
                 ff_depth=64,
                 dropout=0.0,
                ):
        super(CoEvoFormer, self).__init__()

        self.model_depth = model_depth
        self.encoder = Encoder(n_layers=n_layers,
                               n_heads=n_heads,
                               model_depth=model_depth,
                               ff_depth=ff_depth,
                               dropout=dropout,
                               )

        if vocab_size is not None:
            if isinstance(vocab_size, int):
                self.set_vocab_size(vocab_size)

            else:
                self.set_vocab_size(vocab_size[0], vocab_size[1])

    def set_vocab_size(self, src_vocab_size):
        self.src_embedder = Embedding(src_vocab_size, self.model_depth)
        self.generator = Generator(self.model_depth, src_vocab_size)

        for p in self.parameters():
            if p.dim() > 1:
                nn.init.xavier_uniform_(p)

    def forward(self, src, src_mask=None):
        enc_out = self.encoder(self.src_embedder(src), src_mask)

        return enc_out


## (1)coEvoFormer
class CoEvoFormer(nn.Module):
    def __init__(self, model_conf):
        super(CoEvoFormer, self).__init__()
        torch.set_default_dtype(torch.float32)
        self._model_conf = model_conf
        self._msa_conf = model_conf.msa

        self.msa_encoder = CoEvoEmbedder(
                            vocab_size=self._msa_conf.num_msa_vocab,
                            n_layers=self._msa_conf.msa_layers,
                            n_heads=self._msa_conf.msa_heads,
                            model_depth=self._msa_conf.msa_embed_size,
                            ff_depth=self._msa_conf.msa_hidden_size,
                            dropout=self._model_conf.dropout,
                        )

        self.col_attn = MultiHeadAttention(
                num_heads=self._msa_conf.msa_heads,
                embed_dim=self._msa_conf.msa_embed_size,
            )

        self.row_attn = MultiHeadAttention(
                num_heads=self._msa_conf.msa_heads,
                embed_dim=self._msa_conf.msa_embed_size,
            )

```

```python
    def forward(
        self,
        msa_feature,
        msa_mask=None,
    ):
        bs, n_msa, n_token = msa_feature.size()
        msa_feature = msa_feature.reshape(bs*n_msa, n_token)
        msa_embed = self.msa_encoder(msa_feature).reshape(bs, n_msa, n_token, -1)
        msa_embed = msa_embed.transpose(1, 2).reshape(bs*n_token, n_msa, -1)

        if msa_mask is not None:
            msa_mask = msa_mask.transpose(1, 2).reshape(bs*n_token, n_msa)

        msa_embed = self.col_attn(msa_embed, msa_embed, mask=msa_mask).reshape(bs, n_token,
 n_msa, -1).transpose(1, 2)
        msa_embed = msa_embed.reshape(bs*n_msa, n_token, -1)

        if msa_mask is not None:
            msa_mask = msa_mask.reshape(bs, n_token, n_msa)
            msa_mask = msa_mask.transpose(1, 2).reshape(bs*n_msa, n_token)

        msa_embed = self.row_attn(msa_embed, msa_embed, mask=msa_mask).reshape(bs, n_msa,
 n_token, -1)

        return msa_embed
```

Listing 1: Pytorch Implementation of coEvoFormer.

E MOLECULE GNN

E.1 3D MOLECULE GNN

The 3D molecule GNN plays a crucial role in EnzymeFlow. During the structure-based hierarchical pre-training, it encodes ligand molecule representations, learning the constrained geometry between protein binding pockets and ligand molecules. This pre-training process makes the 3D molecule GNN transferable. When the flow model is fine-tuned, the 3D molecule GNN is also fine-tuned, transferring its prior knowledge about ligand molecules to substrate molecules in enzyme-catalyzed reactions. This allows for substrate-specific encodings while leveraging the knowledge learned from protein-ligand interactions.

Consider a molecule l_s with N_{l_s} atoms; this could be a ligand conformation in a protein-ligand pair or a substrate conformation in an enzyme-substrate pair. The molecule l_s can be viewed as a set of atomic point clouds in 3D Euclidean space, where each atom is characterized by its atomic type. There is a distance relationship between each atom pair in the point cloud, which can be processed as bonding features. In our 3D molecule GNN, we use a radial basis function to process these pairwise atomic distances, a technique commonly employed to ensure equivariance and invariance in model design (Hua et al., 2023; Zhang et al., 2024a;b). The 3D molecule GNN takes a molecule conformation l_s as input and outputs an embedded molecule representation $H_{l_s} \in \mathbb{R}^{N_{l_s} \times D_{H_{l_s}}}$, where $D_{H_{l_s}}$ denotes the hidden dimension size.

The code for 3D Molecule GNN follows directly:

```python
import math
import numpy as np

import torch
import torch.nn as nn
from torch.nn import functional as F

## (1)3D Molecule GNN
class MolEmbedder3D(nn.Module):
    def __init__(self, model_conf):
        super(MolEmbedder3D, self).__init__()
        torch.set_default_dtype(torch.float32)
        self._model_conf = model_conf
        self._embed_conf = model_conf.embed

        node_embed_dims = self._model_conf.num_atom_type
        node_embed_size = self._model_conf.node_embed_size
        self.node_embedder = nn.Sequential(
            nn.Embedding(node_embed_dims, node_embed_size, padding_idx=0),
            nn.SiLU(),
            nn.Linear(node_embed_size, node_embed_size),
            nn.LayerNorm(node_embed_size),
            )

        self.node_aggregator = nn.Sequential(
            nn.Linear(node_embed_size + self._model_conf.edge_embed_size, node_embed_size),
            nn.SiLU(),
            nn.Linear(node_embed_size, node_embed_size),
            nn.SiLU(),
            nn.Linear(node_embed_size, node_embed_size),
            nn.LayerNorm(node_embed_size),
            )

        self.dist_min = self._model_conf.ligand_rbf_d_min
        self.dist_max = self._model_conf.ligand_rbf_d_max
        self.num_rbf_size = self._model_conf.num_rbf_size
        self.edge_embed_size = self._model_conf.edge_embed_size

        self.edge_embedder = nn.Sequential(
            nn.Linear(self.num_rbf_size + node_embed_size + node_embed_size, self.
    edge_embed_size),
            nn.SiLU(),
            nn.Linear(self._model_conf.edge_embed_size, self._model_conf.edge_embed_size),
            nn.SiLU(),
            nn.Linear(self._model_conf.edge_embed_size, self._model_conf.edge_embed_size),
            nn.LayerNorm(self._model_conf.edge_embed_size),
            )

        mu = torch.linspace(self.dist_min, self.dist_max, self.num_rbf_size)
        self.mu = mu.reshape([1, 1, 1, -1])

        self.sigma = (self.dist_max - self.dist_min) / self.num_rbf_size

    # Distance function -- pair-wise distance computation
    def coord2dist(self, coord, edge_mask):
        n_batch, n_atom = coord.size(0), coord.size(1)
        radial = torch.sum((coord.unsqueeze(1) - coord.unsqueeze(2)) ** 2, dim=-1)
        dist = torch.sqrt(
                radial + 1e-10
            ) * edge_mask

        radial = radial * edge_mask
        return radial, dist

    # RBF function -- distance encoding
    def rbf(self, dist):
        dist_expand = torch.unsqueeze(dist, -1)
        _mu = self.mu.to(dist.device)
        rbf = torch.exp(-(((dist_expand - _mu) / self.sigma) ** 2))
        return rbf

    def forward(
        self,
        ligand_atom,
        ligand_pos,
        edge_mask,
    ):
        num_batch, num_atom = ligand_atom.shape

        # Atom Embbedding
        node_embed = self.node_embedder(ligand_atom)

        # Edge Feature Computation
        radial, dist = self.coord2dist(
                            coord=ligand_pos,
                            edge_mask=edge_mask,
                        )
        edge_embed = self.rbf(dist) * edge_mask[..., None]
        src_node_embed = node_embed.unsqueeze(1).repeat(1, num_atom, 1, 1)
        tar_node_embed = node_embed.unsqueeze(2).repeat(1, 1, num_atom, 1)
        edge_embed = torch.cat([src_node_embed, tar_node_embed, edge_embed], dim=-1)

        # Edge Embedding
        edge_embed = self.edge_embedder(edge_embed.to(torch.float))

        # Message-Passing
        src_node_agg = (edge_embed.sum(dim=1) / (edge_mask[..., None].sum(dim=1)+1e-10)) *
    ligand_atom.clamp(max=1.)[..., None]
        src_node_agg = torch.cat([node_embed, src_node_agg], dim=-1)

        # Residue Connection
        node_embed = node_embed + self.node_aggregator(src_node_agg)

        return node_embed, edge_embed
```

Listing 2: Pytorch Implementation of 3D Molecule GNN.

E.2 2D Molecule GNN

Like the 3D molecule GNN, the 2D molecule GNN is also important in our EnzymeFlow implementation. In an enzyme-catalyzed reaction, the substrate molecule is transformed into a product molecule, with enzyme-substrate interactions driving this chemical transformation. The 2D molecule GNN plays a key role in modeling and encoding this transformation during the catalytic process, making it equally important as our use of co-evolutionary dynamics. While the 3D molecule GNN encodes the substrate, the 2D molecule GNN encodes the product, guiding the design of the enzyme catalytic pocket.

Consider a product molecule l_p with N_{l_p} atoms in a catalytic reaction. This molecule can be represented as a graph, where nodes correspond to atoms and edges represent bonds. In our 2D molecule GNN, we use fingerprints with attention mechanisms (Xiong et al., 2019) to facilitate message passing between atoms, enabling effective communication across the molecule. The 2D molecule GNN takes this molecular graph l_p as input and outputs an embedded molecule representation $H_{l_p} \in \mathbb{R}^{N_{l_p} \times D_{H_{l_p}}}$, where $D_{H_{l_p}}$ denotes the hidden dimension size.

The code for 2D Molecule GNN follows directly:

```python
import torch
import torch.nn as nn
from torch_geometric.nn.models import AttentiveFP

## (1)2D Molecule GNN
class MolEmbedder2D(nn.Module):
    def __init__(self, model_conf):
        super(MolEmbedder2D, self).__init__()
        torch.set_default_dtype(torch.float32)
        self._model_conf = model_conf

        self.node_embed_dims = self._model_conf.mpnn.mpnn_node_embed_size
        self.edge_embed_dims = self._model_conf.mpnn.mpnn_edge_embed_size

        self.node_embedder = nn.Sequential(
            nn.Embedding(self._model_conf.num_atom_type, self.node_embed_dims),
            nn.SiLU(),
            nn.Linear(self.node_embed_dims, self.node_embed_dims),
            nn.LayerNorm(self.node_embed_dims),
            )

        self.edge_embedder = nn.Sequential(
            nn.Embedding(self._model_conf.mpnn.num_edge_type, self.edge_embed_dims),
            nn.SiLU(),
            nn.Linear(self.edge_embed_dims, self.edge_embed_dims),
            nn.LayerNorm(self.edge_embed_dims),
            )

        # Message Passing with Atttention and Fingerprint
        self.mpnn = AttentiveFP(
                    in_channels=self.node_embed_dims,
                    hidden_channels=self.node_embed_dims,
                    out_channels=self.node_embed_dims,
                    edge_dim=self.edge_embed_dims,
                    num_layers=self._model_conf.mpnn.mpnn_layers,
                    num_timesteps=self._model_conf.mpnn.n_timesteps,
                    dropout=self._model_conf.mpnn.dropout,
                )

    # Dense Edge Matrix to Sparse Edge Matrix
    def dense_to_sparse(
        self,
        mol_atom,
        mol_edge,
        mol_edge_feat,
        mol_atom_mask,
        mol_edge_mask,
    ):
        mol_atom_list = mol_atom[mol_atom_mask]
        mol_edge_feat_list = mol_edge_feat[mol_edge_mask]

        if mol_edge.size(dim=1) == 2:
            mol_edge = mol_edge.transpose(1,2)
        mol_edge_list = [edge[mask] for edge, mask in zip(mol_edge, mol_edge_mask)]

        n_nodes = mol_atom_mask.sum(dim=1, keepdim=True)
        cum_n_nodes = torch.cumsum(n_nodes, dim=0)
        new_mol_edge_list = [mol_edge_list[0]]
        for edge, size in zip(mol_edge_list[1:], cum_n_nodes[:-1]):
            new_mol_edge = edge + size
            new_mol_edge_list.append(new_mol_edge)

        new_mol_edge_list = torch.cat(new_mol_edge_list, dim=0)

        if new_mol_edge_list.size(dim=1) == 2:
            new_mol_edge_list = new_mol_edge_list.transpose(1,0)

        idx = 0
        batch_mask = []
        for size in n_nodes:
            batch_mask.append(torch.zeros(size, dtype=torch.long) + idx)
            idx += 1
        batch_mask = torch.cat(batch_mask).to(mol_atom.device)

        return mol_atom_list, new_mol_edge_list, mol_edge_feat_list, batch_mask

    def forward(
        self,
        mol_atom,
        mol_edge,
        mol_edge_feat,
        mol_atom_mask,
        mol_edge_mask,
    ):
        n_batch = mol_atom.size(0)

        mol_atom_mask = mol_atom_mask.bool()
        mol_edge_mask = mol_edge_mask.bool()
        mol_atom, mol_edge, mol_edge_feat, batch_mask = self.dense_to_sparse(mol_atom,
 mol_edge, mol_edge_feat, mol_atom_mask, mol_edge_mask)
        assert mol_edge.size(1) == mol_edge_feat.size(0)

        # Atom Embedding
        mol_atom = self.node_embedder(mol_atom)

        # Edge Embedding
        mol_edge_feat = self.edge_embedder(mol_edge_feat)

        # Message-Passing
        mol_rep = self.mpnn(mol_atom, mol_edge, mol_edge_feat, batch_mask)

        return mol_rep
```

Listing 3: Pytorch Implementation of 2D Molecule GNN.

F Vector Field Computation and Sampling

Here, we describe how to compute vectors fields and perform sampling for catalytic pocket residues frames, EC-class, as well as the enzyme-reaction co-evolution.

F.1 Background

Catalytic Pocket Frame. We refer to the protein structure as the backbone atomic coordinates of each residue. A pocket of length N_r can be parameterized into SE(3) residue frames $\{(x^i, r^i, c^i)\}_{i=1}^{N_r}$, where $x^i \in \mathbb{R}^3$ represents the position (translation) of the C_α atom of the i-th residue, $r^i \in \mathrm{SO(3)}$ is a rotation matrix defining the local frame relative to a global reference frame, and $c^i \in \{1, \dots, 20\} \cup \{\times\}$ denotes the amino acid type, with additional $\times$ indicating a *masking state* of the amino acid type. We refer to the residue block as $T^i = (x^i, r^i, c^i)$, and the entire pocket is described by a set of residues $\mathbf{T} = \{T^i\}_{i=1}^{N_r}$. Additionally, we denote the graph representations of substrate and product molecules in the catalytic reaction as l_s and l_p, respectively. An enzyme-reaction pair can therefore be described as $(\mathbf{T}, l_s, l_p)$. For simplicity, we omit i.

EC-Class. An EC-class is denoted as $y_{\text{ec}} \in \{1, \dots, 7\} \cup \{\times\}$, with $\times$ indicating the *masking state*.

Co-evolution. The co-evolution of an enzyme-reaction pair is represented by a matrix $U \in \mathbb{R}^{N_{\text{MSA}} \times N_{\text{token}}}$, which combines the MSA results of enzyme sequences and reaction SMILES, where N_{MSA} denotes the number of MSA sequences and N_{token} denotes the length of the MSA alignment preserved. And each element $u^{mn} \in \{1, \ldots, 64\} \cup \{\times\}$ in U denotes a tokenized character from our co-evolution vocabulary, with additional $\times$ indicating the *masking state*.

Vector Field. flow matching describes a process where a flow transforms a simple distribution p_0 into the target data distribution p_1 (Lipman et al., 2022). The goal in flow matching is to train a neural network $v_\theta(\epsilon_t, t)$ that approximates the vector field $u_t(\epsilon)$, which measures the transformation of the distribution $p_t(\epsilon_t)$ as it evolves toward $p_1(\epsilon_t)$ over time $t \in [0, 1)$. The process is optimized using a regression loss defined as $\mathcal{L}_{\text{FM}} = \mathbb{E}_{t\sim\mathcal{U}[0,1],p_t(\epsilon_t)} \|v_\theta(\epsilon_t, t) - u_t(\epsilon)\|^2$. However, directly computing $u_t(\epsilon)$ is often intractable in practice. Instead, a conditional vector field $u_t(\epsilon|\epsilon_1)$ is defined, and the conditional flow matching objective is computed as $\mathcal{L}_{\text{CFM}} = \mathbb{E}_{t\sim\mathcal{U}[0,1],p_t(\epsilon_t)} \|v_\theta(\epsilon_t, t) - u_t(\epsilon|\epsilon_1)\|^2$. Notably, $\nabla_\theta \mathcal{L}_{\text{FM}} = \nabla_\theta \mathcal{L}_{\text{CFM}}$.

During inference or sampling, an ODEsolver, *e.g.*, Euler method, is typically used to solve the ODE governing the flow, expressed as $\epsilon_1 = \texttt{ODEsolver}(\epsilon_0, v_\theta, 0, 1)$, where ϵ_0 is the initial data and ϵ_1 is the generated data. In actual training, rather than directly predicting the vector fields, it is more common to use the neural network to predict the final state at $t = 1$, then interpolates to calculate the vector fields. This approach has been shown to be more efficient and effective for network optimization (Yim et al., 2023a; Bose et al., 2023; Campbell et al., 2024).

F.2 Continuous Variable Trajectory

Given the predictions for translation $\hat{x}_1$ and rotation $\hat{r}_1$ at $t = 1$, we interpolate and their corresponding vector fields are computed as follows:

$$v_\theta(x_t, t) = \frac{\hat{x}_1 - x_t}{1 - t}, \quad v_\theta(r_t, t) = \frac{\log_{r_t} \hat{r}_1}{1 - t}. \tag{9}$$

The sampling or trajectory can then be computed using Euler steps with a step size Δt, as follows:

$$x_{t+\Delta t} = x_t + v_\theta(x_t, t) \cdot \Delta t, \quad r_{t+\Delta t} = r_t + v_\theta(r_t, t) \cdot \Delta t, \tag{10}$$

where the prior of x_0, r_0 are chosen as the uniform distribution on $\mathbb{R}^3$ and SO(3), respectively.

F.3 Discrete Variable Trajectory

For the discrete variables, including amino acid types, EC-class, and co-evolution, we follow Campbell et al. (2024) to use continuous time Markov chains (CTMC).

Continuous Time Markov Chain. A sequence trajectory ϵ_t over time $t \in [0, 1]$ that follows a CTMC alternates between resting in its current state and periodically jumping to another randomly chosen state. The frequency and destination of the jumps are determined by the rate matrix $R_t \in \mathbb{R}^{N\times N}$ with the constraint its off-diagonal elements are non-negative. The probability of ϵ_t jumping to a different state s follows $R_t(\epsilon_t, s)\mathrm{d}t$ for the next infinitesimal time step $\mathrm{d}t$. We can express the transition probability as

$$p_{t+\mathrm{d}t}(s|\epsilon_t) = \delta\{\epsilon_t, s\} + R_t(\epsilon_t, s)\mathrm{d}t, \tag{11}$$

where $\delta(\mathrm{a}, \mathrm{b})$ is the Kronecker delta, equal to 1 if $\mathrm{a} = \mathrm{b}$ and 0 if $\mathrm{a} \neq \mathrm{b}$, and $R_t(\epsilon_t, \epsilon_t) = -\sum_{\gamma\neq\epsilon}(\epsilon_t, \gamma)$ (Campbell et al., 2024). Therefore, $p_{t+\mathrm{d}t}$ is a Categorical distribution with probabilities $\delta(\epsilon_t, \cdot) + R_t(\epsilon_t, \cdot)\mathrm{d}t$ with notation $s \sim \mathrm{Cat}(\delta(\epsilon_t, s) + R_t(\epsilon_t, s)\mathrm{d}t)$.

For finite time intervals Δt, a sequence trajectory can be simulated with Euler steps following:

$$\epsilon_{t+\Delta t} \sim \mathrm{Cat}(\delta(\epsilon_t, \epsilon_{t+\Delta t}) + R_t(\epsilon_t, \epsilon_{t+\Delta t})\Delta t). \tag{12}$$

The rate matrix R_t along with an initial distribution p_0 define CTMC. Furthermore, the probability flow p_t is the marginal distribution of ϵ_t at every time t, and we say the rate matrix R_t generates p_t if $\partial_t p_t = R_t^T p_t, \forall t \in [0, 1]$.

In the actual training, Campbell et al. (2024) show that we can train a neural network to approximate the true denoising distribution using the standard cross-entropy:

$$\mathcal{L}_{\text{CE}} = \mathbb{E}_{t\sim\mathcal{U}[0,1],p_t(\epsilon_t)}[\log p_\theta(\epsilon_1|\epsilon_t)], \tag{13}$$

which leads to our neural network objectives for amino acid types, EC-class, and co-evolution as:

$$\begin{aligned}&\mathcal{L}_{\text{aa}} = \mathbb{E}_{t\sim\mathcal{U}[0,1],p_t(c_t)}[\log p_\theta(c_1|c_t)], \mathcal{L}_{\text{ec}} = \mathbb{E}_{t\sim\mathcal{U}[0,1],p_t(y_{\text{ec}_t})}[\log p_\theta(y_{\text{ec}_1}|y_{\text{ec}_t})],\\ &\mathcal{L}_{\text{coevo}} = \mathbb{E}_{t\sim\mathcal{U}[0,1],p_t(u_t)}[\log p_\theta(u_1|u_t)].\end{aligned} \tag{14}$$

Rate Matrix for Inference. The conditional rate matrix $R_t(\epsilon_t, s|s_1)$ generates the conditional flow $p_t(\epsilon_t|\epsilon_1)$. And $R_t(\epsilon_t, s) = \mathbb{E}_{p_1(\epsilon_1|\epsilon_t)}[R_t(\epsilon_t, s|\epsilon_1)]$, for which the expectation is taken over $p_1(\epsilon_1|\epsilon_t) = \frac{p_t(\epsilon_t|\epsilon_1)p_1(\epsilon_1)}{p_t(\epsilon_t)}$. With the conditional rate matrix, the sampling can be performed:

$$\begin{aligned}&R_t(\epsilon_t,\cdot) \leftarrow \mathbb{E}_{p_1(\epsilon_1|\epsilon_t)}[R_t(\epsilon_t,\cdot|\epsilon_1)],\\ &\epsilon_{t+\Delta t} \sim \text{Cat}(\delta(\epsilon_t,\epsilon_{t+\Delta t}) + R_t(\epsilon_t,\epsilon_{t+\Delta t})\Delta t).\end{aligned} \tag{15}$$

The rate matrix generates the probability flow for discrete variables.

Campbell et al. (2024) define the conditional rate matrix starting with

$$R_t(\epsilon_t, s|\epsilon_t) = \frac{\text{ReLU}(\partial_t p_t(s|\epsilon_1) - \partial_t p_t(\epsilon_t|\epsilon_1))}{N\cdot p_t(\epsilon_t|\epsilon_1)}. \tag{16}$$

In practice, the closed-form of conditional rate matrix with *masking state* $\times$ is defined as:

$$R_t(\epsilon_t, s|\epsilon_1) = \frac{\delta(\epsilon_1, s)}{1-t}\delta(\epsilon_t, \times). \tag{17}$$

With the definition of the conditional rate matrix $R_t(\epsilon_t, s|\epsilon_1)$, we can perform sampling and inference for amino acid types, EC-class, and co-evolution following:

$$\begin{aligned}&c_{t+\Delta t} \sim \text{Cat}(\delta(c_t, c_{t+\Delta t}) + R_t(c_t, c_{t+\Delta t}|v_\theta(c_t,t))\cdot\Delta t),\\ &y_{\text{ec}_{t+\Delta t}} \sim \text{Cat}(\delta(y_{\text{ec}_t}, y_{\text{ec}_{t+\Delta t}}) + R_t(y_{\text{ec}_t}, y_{\text{ec}_{t+\Delta t}}|v_\theta(y_{\text{ec}_t},t))\cdot\Delta t),\\ &u_{t+\Delta t} \sim \text{Cat}(\delta(u_t, u_{t+\Delta t}) + R_t(u_t, u_{t+\Delta t}|v_\theta(u_t,t))\cdot\Delta t).\end{aligned} \tag{18}$$

G EnzymeFlow SE(3)-equivariance

Theorem. *Let ϕ denote an SE(3) transformation. The catalytic pocket design in EnzymeFlow, represented as $p_\theta(\mathbf{T}|l_s)$, is SE(3)-equivariant, meaning that $p_\theta(\phi(\mathbf{T})|\phi(l_s)) = p_\theta(\mathbf{T}|l_s)$, where $\mathbf{T}$ represents the generated catalytic pocket, and l_s denotes the substrate conformation.*

Proof. Given an SE(3)-invariant prior, such that $p(\mathbf{T}_0, l_s) = p(\phi(\mathbf{T}_0), \phi(l_s))$, and an SE(3)-equivariant transition state for each time step t via an SE(3)-equivariant neural network, such that $p_\theta(\mathbf{T}_{t+\Delta t}, l_s) = p_\theta(\phi(\mathbf{T}_{t+\Delta t}), \phi(l_s))$, it follows that for the total time steps T, we have:

$$\begin{aligned}p_\theta(\phi(\mathbf{T}_1)|\phi(l_s)) &= \int p_\theta(\phi(\mathbf{T}_0, l_s))\prod_{n=0}^{T-1} p_\theta(\phi(\mathbf{T}_{n\Delta t+\Delta t}, l_s)|\phi(\mathbf{T}_{n\Delta t}, l_s))\\ &= \int p_\theta(\mathbf{T}_0, l_s)\prod_{n=0}^{T-1} p_\theta(\phi(\mathbf{T}_{n\Delta t+\Delta t}, l_s)|\phi(\mathbf{T}_{n\Delta t}, l_s))\\ &= \int p_\theta(\mathbf{T}_0, l_s)\prod_{n=0}^{T-1} p_\theta(\mathbf{T}_{n\Delta t+\Delta t}, l_s|\mathbf{T}_{n\Delta t}, l_s)\\ &= p_\theta(\mathbf{T}_1|l_s).\end{aligned} \tag{19}$$

□

H EnzymeFlow Dataset Statistics

Data Source. We construct a curated and validated dataset of enzyme-reaction pairs by collecting data from the Rhea (Bansal et al., 2022), MetaCyc (Caspi et al., 2020), and Brenda (Schomburg et al., 2002) databases. For enzymes in these databases, we exclude entries missing UniProt IDs or protein sequences. For reactions, we apply the following procedures: (1) remove cofactors, small

Data	Reaction	Enzyme	Substrate		Product		Enzyme Commission Class						
	#reaction	#enzyme	#substrate	#avg atom	#product	#avg atom	EC1	EC2	EC3	EC4	EC5	EC6	EC7
Rawdata	232520	97912	7259	30.81	7664	30.34	44881 (19.30%)	75944 (32.66%)	37728 (16.23%)	47242 (20.32%)	8315 (3.58%)	18281 (7.86%)	129 (0.06%)
40% Homo	19379	6922	4798	31.06	4897	30.24	4754 (24.53%)	5857 (30.22%)	4839 (24.97%)	1764 (9.10%)	759 (3.92%)	1379 (7.12%)	27 (0.14%)
50% Homo	34750	13442	5675	31.45	5871	30.75	8184 (23.55%)	11174 (32.16%)	8050 (23.17%)	3203 (9.22%)	1357 (3.91%)	2752 (7.92%)	30 (0.09%)
60% Homo	53483	22350	6112	30.95	6331	30.34	11674 (21.83%)	18419 (34.44%)	11394 (21.30%)	5555 (10.39%)	2194 (4.10%)	4200 (7.85%)	47 (0.09%)
80% Homo	100925	43458	6619	30.46	6943	29.95	21308 (21.11%)	34344 (34.03%)	18925 (18.75%)	14010 (13.88%)	3901 (3.87%)	8371 (8.29%)	66 (0.07%)
90% Homo	132047	55697	6928	30.32	7298	29.81	28833 (21.84%)	43287 (32.78%)	23989 (18.17%)	20070 (15.20%)	5015 (3.80%)	10766 (8.15%)	87 (0.07%)

Table 3: EnzymeFill Dataset Statistics.

Data	Reaction	Enzyme	Substrate		Product		Enzyme Commision						
	#reaction	#enzyme	#substrate	#avg atom	#product	#avg atom	EC1	EC2	EC3	EC4	EC5	EC6	EC7
Rawdata	232520	97912	7259	30.81	7664	30.34	44881 (19.30)	75944 (32.66)	37728 (16.23)	47242 (20.32)	8315 (3.58)	18281 (7.86)	129 (0.06)
Train Data	53483	22350	6112	30.95	6331	30.34	11674 (21.83)	18419 (34.44)	11394 (21.30)	5555 (10.39)	2194 (4.10)	4200 (7.85)	47 (0.09)
Eval Data	100	100	100	30.7	94	28.84	17 (17.00)	17 (17.00)	17 (17.00)	17 (17.00)	16 (16.00)	16 (16.00)	0 (0.00)

Table 4: EnzymeFlow Evaluation Data Statistics.

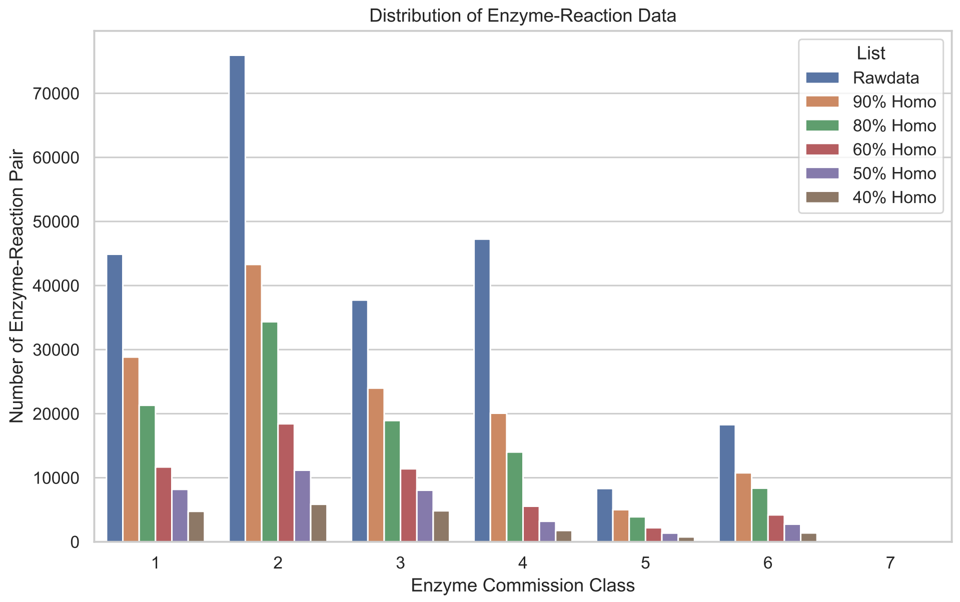

Figure 11: Distribution of enzyme-reaction pairs over EC-class.

ion groups, and molecules that appear in both substrates and products within a single reaction; (2) exclude reactions with more than five substrates or products; and (3) apply OpenBabel (O'Boyle et al., 2011) to standardize molecular SMILES. Ultimately, we obatin a total of $328,192$ enzyme-reaction pairs, comprising $145,782$ unique enzymes and $17,868$ unique reactions.

Debiasing. To ensure the quality of catalytic pocket data, we exclude pockets with fewer than 32 residues, resulting in $232,520$ enzyme-reaction pairs. Additionally, enzymes and their catalytic pockets can exhibit significant sequence similarity. When enzymes that are highly similar in sequence appear too frequently in the dataset, they tend to belong to the same cluster or homologous group, which can introduce substantial biases during model training. To mitigate this issue and ensure a more balanced dataset, it is important to reduce the number of homologous enzymes by clustering and selectively removing enzymes from the same clusters. This helps to debias the data and improve the model's generalizability. We perform sequence alignment to cluster enzymes and identify homologous ones (Steinegger & Söding, 2017). We then revise the dataset into five major categories based on enzyme sequence similarity, resulting in: (1) $19,379$ pairs with at most 40% homology, (2) $34,750$ pairs with at most 50% homology, (3) $53,483$ pairs with at most 60% homology, (4) $100,925$ pairs with at most 80% homology, and (5) $132,047$ pairs with at most 90% homology. We provide data statistics, including the EC-class distribution, in Table 3, and visualize the distribution in Figure 11.

From the data, we observe that EC1, EC2, EC3, and EC4 contribute the most enzyme-reaction pairs to our dataset. Specifically, EC1 refers to oxidation/reduction reactions, involving the transfer of hydrogen, oxygen atoms, or electrons from one substance to another. EC2 involves the transfer of a functional group (such as methyl, acyl, amino, or phosphate) from one substance to another. EC3 is associated with the formation of two products from a substrate through hydrolysis, while EC4 involves the non-hydrolytic addition or removal of groups from substrates, potentially cleaving C-C, C-N, C-O, or C-S bonds. Our dataset distribution closely follows the natural enzyme-reaction enzyme commission class distribution, with Transferases (EC2) being the most dominant.

I Work in Progress: Enzyme Pocket-Reaction Recruitment with Enzyme CLIP Model

In addition to evaluating the catalytic pockets generated from the functional and structural perspectives, we may raise a key question of how we *quantitatively* determine whether the generated pockets can catalyze a specific reaction. To answer it, we are working to train an enzyme-reaction CLIP model using enzyme-reaction pairs (with pocket-specific information) from the 60%-clustered data, excluding the 100 evaluation samples from training. All enzymes not annotated to catalyze a specific reaction are treated as negative samples, following the approach in Yang et al. (2024); Mikhael et al. (2024). For the 100 generated catalytic pockets of each reaction, we select the `Top-1` pocket with the highest `TM-score` for evaluation using the enzyme CLIP model.

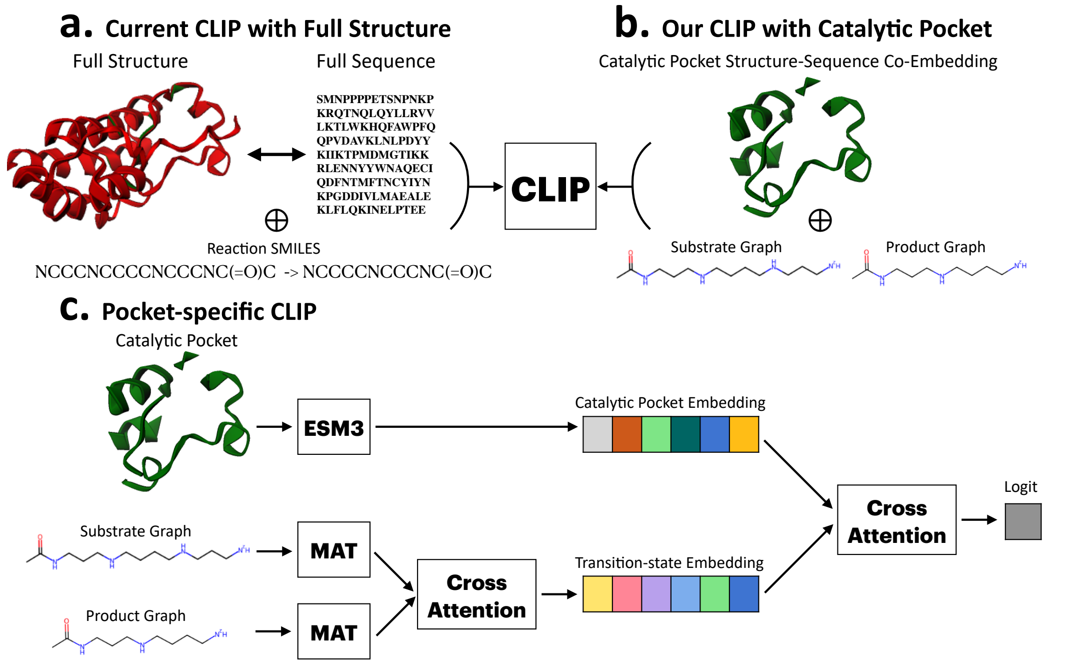

Figure 12: Enzyme-Reaction CLIP model comparison. (a) Existing CLIP models use the full enzyme structure or full enzyme sequence, paired with reaction SMILES as input. (b) Our pocket-specific CLIP model focuses on catalytic pockets, using both their structures and sequences paired with molecular graphs of reactions. The pocket-specific CLIP approach learns from enzyme active sites, which exhibit higher functional concentration. (c) Overview of Pocket-specific CLIP model.

Pocket-specific CLIP. Unlike existing methods that typically train on full enzyme structures or sequences (Yu et al., 2023; Mikhael et al., 2024), our pocket-specific CLIP approach is designed to focus specifically on catalytic pockets, including both their structures and sequences, paired with molecular graphs of catalytic reactions (illustrated in Fig. 12). As shown in Fig. 2(b), catalytic pockets are usually the regions that exhibit high functional concentration, while the remaining parts tend to be less functionally important. Therefore, focusing on catalytic pockets is more applicable and effective for enzyme CLIP models. The advantage of the pocket-specific CLIP is that it learns from active sites that are highly meaningful both structurally and sequentially.

We illustrate our pocket-specific enzyme CLIP approach in Fig. 12. In our pocket-specific CLIP model, we encode the pocket structure and sequence using ESM3 (Hayes et al., 2024), and the substrate and product molecular graphs using MAT (Maziarka et al., 2020). Cross-attention is applied to compute the transition state of the reaction, capturing the transformation of the substrate into the product, as proposed in Hua et al. (2024b). This is followed by another cross-attention mechanism to learn the interactions between the catalytic pocket and the reaction. The model is trained by enforcing high logits for positive enzyme-reaction pairs and low logits for negative enzyme-reaction pairs.

Metrics. To evaluate the catalytic ability of the designed pockets for a given reaction, we employ retrieval-based ranking as proposed in Hua et al. (2024b). This ranking-based evaluation ensures fairness and minimizes biases. The metrics include: `Top-k Acc`, which quantifies the proportion of instances in which the catalytic pocket is ranked within the CLIP's top-k predictions; `Mean Rank`, which calculates the average position of the pocket in the retrieval list; Mean Reciprocal Rank (`MRR`), which measures how quickly the pocket is retrieved by averaging the reciprocal ranks of the first correct pocket across all reactions. These metrics help assess whether a catalytic pocket designed for a specific reaction ranks highly in the recruitment list, indicating its potential to catalyze the reaction.

I.1 Inpainting Catalytic Pocket with ESM3 for Full Enzyme Recruitment

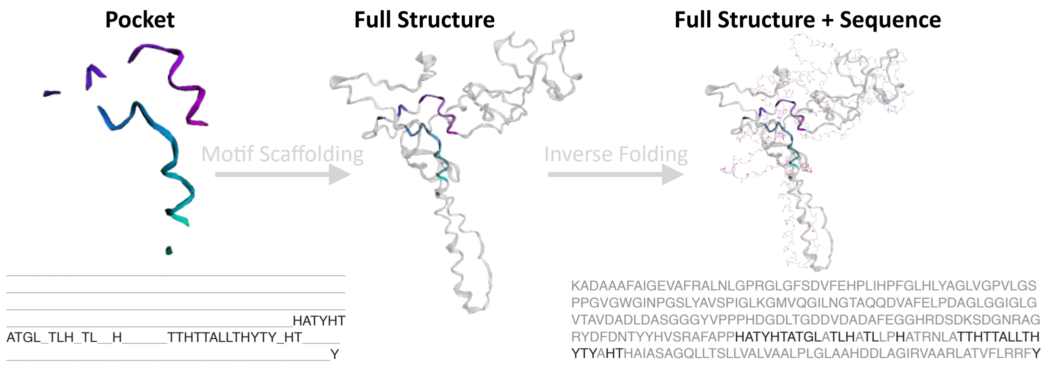
Pocket
Full Structure
Full Structure + Sequence
Motif Scaffolding
Inverse Folding
HATYHT
ATGL_TLH_TL__H______TTHTTALLTHYTY_HT_____
Y
KADAAAFAIGEVAFRALNLGPRGLGFSDVFEHPLIHPFGLHLYAGLVGPVLGS
PPGVGWGINPGSLYAVSPIGLKGMVQGILNGTAQQDVAFELPDAGLGGIGLG
VTAVDADLDASGGGYVPPPHDGDLTGDDVDADAFEGGHRDSDKSDGNRAG
RYDFDNTYYHVSRAFAPPHATYHTATGLATLHATLLPHATRNLATTHTTALLTH
YTYAHTHAIASAGQLLTSLLVALVAALPLGLAAHDDLAGIRVAARLATVFLRRFY

Figure 13: Inpainting catalytic pocket using ESM3.

ESM3 (Hayes et al., 2024) can inpaint missing structures and sequences with functional motifs. In this context, we train a separate full enzyme CLIP model for the enzyme recruitment task. This model is trained using the same 60%-clustered data but incorporates full enzyme structures and sequences. For generated catalytic pockets and those in the evaluation set, we use ESM3 to inpaint them, completing the structures and sequences predicted by ESM3. These ESM3-inpainted enzymes are then evaluated using the full enzyme CLIP model, applying the same retrieval-based ranking metrics as before. We illustrate the catalytic pocket inpainting pipeline in Fig. 13.

In conclusion, we are developing a pocket-specific enzyme CLIP model for pocket-based enzyme recruitment tasks and a full-enzyme CLIP model using ESM3 for inpainting and pocket scaffolding in full enzyme recruitment tasks. However, we recognize that directly using ESM3 for catalytic pocket inpainting lacks domain-specific knowledge, making fine-tuning necessary. To address this, we are working on a fine-tuning open-source large biological model, *e.g.,* Genie2 (Lin et al., 2024), on our EnzymeFill dataset. Genie2, pre-trained on FoldSeek-clustered AlphaFold- and Protein-DataBank proteins for *de novo* protein design and (multi-)motif scaffolding, aligns well with our catalytic pocket scaffolding task. Fine-tuning Genie2 on EnzymeFill will enhance its performance in catalytic pocket inpainting. The development of EnzymeFlow, aimed at achieving an AI-driven automated enzyme design platform, is discussed in App. A.

J RFDiffusionAA-design vs. EnzymeFlow-design

In Fig. 14, we visualize and compare the RFDiffusionAA-generated pockets (Krishna et al., 2024) with EnzymeFlow-generated catalytic pockets, both aligned to the ground-truth reference pockets. In RFDiffusionAA, the generation is conditioned on the substrate conformation, and the pocket sequence is computed post hoc using LigandMPNN (Dauparas et al., 2023). In contrast, EnzymeFlow conditions the generation on the reaction, with the pocket sequence co-designed alongside the pocket structure. In addition to visualization, we report `TM-score`, `RMSD`, and `AAR`, where EnzymeFlow outperforms RFDiffusionAA across all three metrics, demonstrating EnzymeFlow's ability to generate more structurally valid enzyme catalytic pockets.

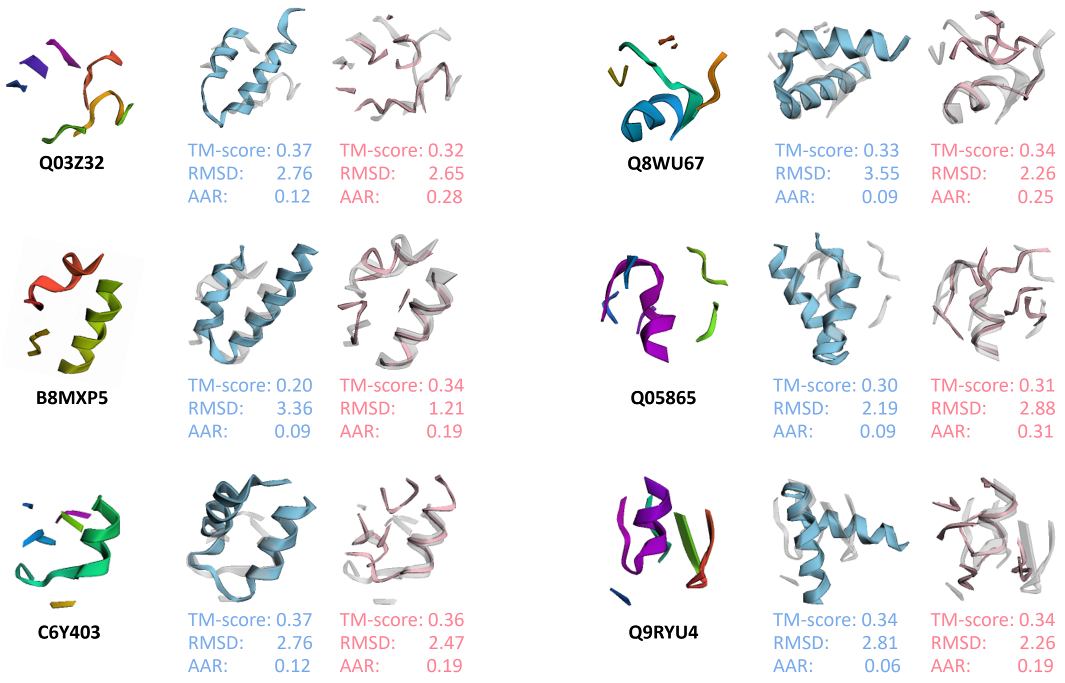

Figure 14: Visualization and comparison between RFDiffusionAA-designed pockets and EnzymeFlow-designed pockets after superimposition with ground-truth pockets. Light color represents EnzymeFlow-designed pockets, blue color represents RFDiffusionAA-designed pockets, spectral color represents the ground-truth reference pockets. `TM-score`, `RMSD`, `AAR` are reported.

K ENZYMEFLOW NEURAL NETWORK IMPLEMENTATION

The equivariant neural network is based on the Invariant Point Attention (IPA) implemented in AlphaFold2 (Jumper et al., 2021). In the following, we detail how enzyme catalytic pockets, substrate molecules, product molecules, EC-class, and co-evolution interact within our network.

The code for EnzymeFlow main network follows directly:

```python
import functools as fn
import math

import torch
import torch.nn as nn
from torch.nn import functional as F

from ofold.utils.rigid_utils import Rigid

from model import ipa_pytorch
from flowmatch.data import all_atom
from flowmatch.data import utils as du

## EnzymeFlow Main Network

## (8) Distogram
def calc_distogram(pos, min_bin, max_bin, num_bins):
    dists_2d = torch.linalg.norm(pos[:, :, None, :] - pos[:, None, :, :], axis=-1)[
        ..., None
    ]
    lower = torch.linspace(min_bin, max_bin, num_bins, device=pos.device)
    upper = torch.cat([lower[1:], lower.new_tensor([1e8])], dim=-1)
    dgram = ((dists_2d > lower) * (dists_2d < upper)).type(pos.dtype)
    return dgram


## (7) Index Embedding
def get_index_embedding(indices, embed_size, max_len=2056):
    K = torch.arange(embed_size // 2, device=indices.device)
    pos_embedding_sin = torch.sin(
        indices[..., None] * math.pi / (max_len ** (2 * K[None] / embed_size))
    ).to(indices.device)
    pos_embedding_cos = torch.cos(
        indices[..., None] * math.pi / (max_len ** (2 * K[None] / embed_size))
    ).to(indices.device)
    pos_embedding = torch.cat([pos_embedding_sin, pos_embedding_cos], axis=-1)
    return pos_embedding


## (6) Time Embedding
def get_timestep_embedding(timesteps, embedding_dim, max_positions=10000):
    assert len(timesteps.shape) == 1
    timesteps = timesteps * max_positions
    half_dim = embedding_dim // 2
    emb = math.log(max_positions) / (half_dim - 1)
    emb = torch.exp(
        torch.arange(half_dim, dtype=torch.float32, device=timesteps.device) * -emb
    )
    emb = timesteps.float()[:, None] * emb[None, :]
    emb = torch.cat([torch.sin(emb), torch.cos(emb)], dim=1)
    if embedding_dim % 2 == 1:  # zero pad
        emb = F.pad(emb, (0, 1), mode="constant")
    assert emb.shape == (timesteps.shape[0], embedding_dim)
    return emb


## (5) Edge Feature Network
class EdgeFeatureNet(nn.Module):
    def __init__(self, module_cfg):
        super(EdgeFeatureNet, self).__init__()
        self._cfg = module_cfg

        self.c_s = self._cfg.embed.c_s
        self.c_z = self._cfg.embed.c_z
        self.feat_dim = self._cfg.embed.feat_dim

        self.linear_s_p = nn.Linear(self.c_s, self.feat_dim)
        self.linear_relpos = nn.Linear(self.feat_dim, self.feat_dim)

        total_edge_feats = self.feat_dim * 3 + self._cfg.embed.num_bins * 2 + 2

        self.edge_embedder = nn.Sequential(
            nn.Linear(total_edge_feats, self.c_z),
            nn.ReLU(),
            nn.Linear(self.c_z, self.c_z),
            nn.ReLU(),
            nn.Linear(self.c_z, self.c_z),
            nn.LayerNorm(self.c_z),
        )

    def embed_relpos(self, r):
        d = r[:, :, None] - r[:, None, :]
        pos_emb = get_index_embedding(d, self.feat_dim, max_len=2056)
        return self.linear_relpos(pos_emb)

    def _cross_concat(self, feats_1d, num_batch, num_res):
        return torch.cat([
            torch.tile(feats_1d[:, :, None, :], (1, 1, num_res, 1)),
            torch.tile(feats_1d[:, None, :, :], (1, num_res, 1, 1)),
        ], dim=-1).float().reshape([num_batch, num_res, num_res, -1])

    def forward(self, s, t, sc_t, edge_mask, flow_mask):
        # Input: [b, n_res, c_s]
        num_batch, num_res, _ = s.shape

        # [b, n_res, c_z]
        p_i = self.linear_s_p(s)
        cross_node_feats = self._cross_concat(p_i, num_batch, num_res)

        # [b, n_res]
        r = torch.arange(
            num_res, device=s.device).unsqueeze(0).repeat(num_batch, 1)
        relpos_feats = self.embed_relpos(r)

        dist_feats = calc_distogram(
            t, min_bin=1e-3, max_bin=20.0, num_bins=self._cfg.embed.num_bins)
        sc_feats = calc_distogram(
            sc_t, min_bin=1e-3, max_bin=20.0, num_bins=self._cfg.embed.num_bins)

        all_edge_feats = [cross_node_feats, relpos_feats, dist_feats, sc_feats]

        diff_feat = self._cross_concat(flow_mask[..., None], num_batch, num_res)
        all_edge_feats.append(diff_feat)

        edge_feats = self.edge_embedder(torch.concat(all_edge_feats, dim=-1).to(torch.float))
        edge_feats *= edge_mask.unsqueeze(-1)
        return edge_feats


## (4) Node Feature Network
class NodeFeatureNet(nn.Module):
    def __init__(self, module_cfg):
        super(NodeFeatureNet, self).__init__()
        self._cfg = module_cfg
        self.c_s = self._cfg.embed.c_s
        self.c_pos_emb = self._cfg.embed.c_pos_emb
        self.c_timestep_emb = self._cfg.embed.c_timestep_emb
        embed_size = self.c_pos_emb + self.c_timestep_emb * 2 + 1

        self.aatype_embedding = nn.Embedding(21, self.c_s) # Always 21 because of 20 amino
     acids + 1 for unk
        embed_size += self.c_s + self.c_timestep_emb + self._cfg.num_aa_type

        self.linear = nn.Sequential(
            nn.Linear(embed_size, self.c_s),
            nn.ReLU(),
            nn.Linear(self.c_s, self.c_s),
            nn.ReLU(),
            nn.Linear(self.c_s, self.c_s),
            nn.LayerNorm(self.c_s),
        )

    def embed_t(self, timesteps, mask):
        timestep_emb = get_timestep_embedding(
            timesteps,
            self.c_timestep_emb,
            max_positions=2056
        )[:, None, :].repeat(1, mask.shape[1], 1)
        return timestep_emb * mask.unsqueeze(-1)

    def forward(
            self,
            *,
            t,
            res_mask,
            flow_mask,
            pos,
            aatypes,
            aatypes_sc,
        ):
        # [b, n_res, c_pos_emb]
        pos_emb = get_index_embedding(pos, self.c_pos_emb, max_len=2056)
        pos_emb = pos_emb * res_mask.unsqueeze(-1)

        # [b, n_res, c_timestep_emb]
        input_feats = [
            pos_emb,
            flow_mask[..., None],
            self.embed_t(t, res_mask),
            self.embed_t(t, res_mask)
        ]
        input_feats.append(self.aatype_embedding(aatypes))
        input_feats.append(self.embed_t(t, res_mask))
        input_feats.append(aatypes_sc)
        return self.linear(torch.cat(input_feats, dim=-1))


## (3) Distance Embedder
class DistEmbedder(nn.Module):
    def __init__(self, model_conf):
        super(DistEmbedder, self).__init__()
        torch.set_default_dtype(torch.float32)
        self._model_conf = model_conf
        self._embed_conf = model_conf.embed

        edge_embed_size = self._model_conf.edge_embed_size

        self.dist_min = self._model_conf.bb_ligand_rbf_d_min
        self.dist_max = self._model_conf.bb_ligand_rbf_d_max
        self.num_rbf_size = self._model_conf.num_rbf_size
        self.edge_embedder = nn.Sequential(
            nn.Linear(self.num_rbf_size, edge_embed_size),
            nn.ReLU(),
            nn.Linear(edge_embed_size, edge_embed_size),
            nn.ReLU(),
            nn.Linear(edge_embed_size, edge_embed_size),
            nn.LayerNorm(edge_embed_size),
        )

        mu = torch.linspace(self.dist_min, self.dist_max, self.num_rbf_size)
        self.mu = mu.reshape([1, 1, 1, -1])
        self.sigma = (self.dist_max - self.dist_min) / self.num_rbf_size

    def coord2dist(self, coord, edge_mask):
        n_batch, n_atom = coord.size(0), coord.size(1)
        radial = torch.sum((coord.unsqueeze(1) - coord.unsqueeze(2)) ** 2, dim=-1)
        dist = torch.sqrt(
                radial + 1e-10
            ) * edge_mask

        radial = radial * edge_mask
        return radial, dist

    def rbf(self, dist):
        dist_expand = torch.unsqueeze(dist, -1)
        _mu = self.mu.to(dist.device)
        rbf = torch.exp(-(((dist_expand - _mu) / self.sigma) ** 2))
        return rbf

    def forward(
        self,
        rigid,
        ligand_pos,
        bb_ligand_mask,
    ):
        curr_bb_pos = all_atom.to_atom37(Rigid.from_tensor_7(torch.clone(rigid)))[-1][:, :,
     1].to(ligand_pos.device)

        curr_bb_lig_pos = torch.cat([curr_bb_pos, ligand_pos], dim=1)
        edge_mask = bb_ligand_mask.unsqueeze(dim=1) * bb_ligand_mask.unsqueeze(dim=2)

        radial, dist = self.coord2dist(
                            coord=curr_bb_lig_pos,
                            edge_mask=edge_mask,
                        )


        edge_embed = self.rbf(dist) * edge_mask[..., None]
        edge_embed = self.edge_embedder(edge_embed.to(torch.float))

        return edge_embed


## (2) Cross-Attentiom
class CrossAttention(nn.Module):
    def __init__(self, query_input_dim, key_input_dim, output_dim):
        super(CrossAttention, self).__init__()
        self.out_dim = output_dim
        self.W_Q = nn.Linear(query_input_dim, output_dim)
        self.W_K = nn.Linear(key_input_dim, output_dim)
        self.W_V = nn.Linear(key_input_dim, output_dim)
        self.scale_val = self.out_dim ** 0.5
        self.softmax = nn.Softmax(dim=-1)

    def forward(self, query_input, key_input, value_input, query_input_mask=None,
     key_input_mask=None):
        query = self.W_Q(query_input)
        key = self.W_K(key_input)
        value = self.W_V(value_input)

        attn_weights = torch.matmul(query, key.transpose(1, 2)) / self.scale_val
        attn_mask = query_input_mask.unsqueeze(-1) * key_input_mask.unsqueeze(-1).transpose(1,
      2)
        attn_weights = attn_weights.masked_fill(attn_mask == False, -1e9)
        attn_weights = self.softmax(attn_weights)
        output = torch.matmul(attn_weights, value)

        return output, attn_weights


## (1) Protein-Ligand Network
class ProteinLigandNetwork(nn.Module):
    def __init__(self, model_conf):
        super(ProteinLigandNetwork, self).__init__()
        torch.set_default_dtype(torch.float32)
        self._model_conf = model_conf

        # Input Node Embedder
        self.node_feature_net = NodeFeatureNet(model_conf)

        # Input Edge Embedder
        self.edge_feature_net = EdgeFeatureNet(model_conf)

        # 3D Molecule GNN
        self.mol_embedding_layer = MolEmbedder(model_conf)

        # Invariant Point Attention (IPA) Network
        self.ipanet = ipa_pytorch.IpaNetwork(model_conf)

        # Node Fusion
        self.node_embed_size = self._model_conf.node_embed_size
        self.node_embedder = nn.Sequential(
            nn.Embedding(self._model_conf.num_aa_type, self.node_embed_size),
            nn.ReLU(),
            nn.Linear(self.node_embed_size, self.node_embed_size),
            nn.LayerNorm(self.node_embed_size),
        )
        self.node_fusion = nn.Sequential(
            nn.Linear(self.node_embed_size + self.node_embed_size, self.node_embed_size),
            nn.ReLU(),
            nn.Linear(self.node_embed_size, self.node_embed_size),
            nn.LayerNorm(self.node_embed_size),
        )

        # Backbone-Substrate Fusion
        self.bb_lig_fusion = CrossAttention(
                query_input_dim=self.node_embed_size,
                key_input_dim=self.node_embed_size,
                output_dim=self.node_embed_size,
        )

        # Edge Fusion
        self.edge_embed_size = self._model_conf.edge_embed_size
        self.edge_dist_embedder = DistEmbedder(model_conf)

        # Amino Acid Prediction Network
        self.aatype_pred_net = nn.Sequential(
                nn.Linear(self.node_embed_size, self.node_embed_size),
                nn.ReLU(),
                nn.Linear(self.node_embed_size, self.node_embed_size),
                nn.ReLU(),
                nn.Linear(self.node_embed_size, model_conf.num_aa_type),
        )

        if self._model_conf.flow_msa:
            # Co-Evolution Embedder
            self.msa_embedding_layer = CoEvoFormer(model_conf)

            # Coevo-Backbone-Substrate Fusion
            self.msa_bb_lig_fusion = CrossAttention(
                query_input_dim=model_conf.msa.msa_embed_size,
                key_input_dim=self.node_embed_size,
                output_dim=self.node_embed_size,
            )

            # Coevo Prediction Network
            self.msa_pred = nn.Sequential(
                nn.Linear(self.node_embed_size, self.node_embed_size),
                nn.SiLU(),
                nn.Linear(self.node_embed_size, self.node_embed_size),
                nn.SiLU(),
                nn.Linear(self.node_embed_size, model_conf.msa.num_msa_vocab),
            )

        if self._model_conf.ec:
            # EC Embedder
            self.ec_embedding_layer = nn.Sequential(
                nn.Embedding(model_conf.ec.num_ec_class, model_conf.ec.ec_embed_size),
                nn.SiLU(),
                nn.Linear(model_conf.ec.ec_embed_size, model_conf.ec.ec_embed_size),
                nn.LayerNorm(model_conf.ec.ec_embed_size),
            )

            # EC-Backbone-Substrate Fusion
            self.ec_bb_lig_fusion = CrossAttention(
                query_input_dim=model_conf.ec.ec_embed_size,
                key_input_dim=self.node_embed_size,
                output_dim=self.node_embed_size,
            )

            # EC Prediction Network
            self.ec_pred = nn.Sequential(
                nn.Linear(self.node_embed_size, self.node_embed_size),
                nn.SiLU(),
                nn.Linear(self.node_embed_size, self.node_embed_size),
                nn.SiLU(),
                nn.Linear(self.node_embed_size, model_conf.ec.num_ec_class),
            )

        self.condition_generation = self._model_conf.guide_by_condition
        if self.condition_generation:
            # 2D Molecule GNN
            self.guide_ligand_mpnn = MolEmbedder2D(model_conf)

            # Backbone-Product Fusion
            self.guide_bb_lig_fusion = CrossAttention(
                query_input_dim=self.node_embed_size,
                key_input_dim=self.node_embed_size,
                output_dim=self.node_embed_size,
            )

    def forward(self, input_feats, use_context=False):
        # Frames as [batch, res, 7] tensors.
        bb_mask = input_feats["res_mask"].type(torch.float32)  # [B, N]
        flow_mask = input_feats["flow_mask"].type(torch.float32)
        edge_mask = bb_mask[..., None] * bb_mask[..., None, :]

        n_batch, n_res = bb_mask.shape

        # Encode Backbone Nodes with Input Node Embedder
        init_bb_node_embed = self.node_feature_net(
            t=input_feats["t"],
            res_mask=bb_mask,
            flow_mask=flow_mask,
            pos=input_feats["seq_idx"],
            aatypes=input_feats["aatype_t"],
            aatypes_sc=input_feats["sc_aa_t"],
        )

        # Encode Backbone Edges with Input Edge Embedder
        init_bb_edge_embed = self.edge_feature_net(
            s=init_bb_node_embed,
            t=input_feats["trans_t"],
            sc_t=input_feats["sc_ca_t"],
            edge_mask=edge_mask,
            flow_mask=flow_mask,
        )

        # Masking Padded Residues
        bb_node_embed = init_bb_node_embed * bb_mask[..., None]
        bb_edge_embed = init_bb_edge_embed * edge_mask[..., None]

        # AminoAcid embedding
        bb_aa_embed = self.node_embedder(input_feats["aatype_t"]) * bb_mask[..., None]
        bb_aa_embed = torch.cat([bb_aa_embed, bb_node_embed], dim=-1)
        # Backbone-AminoAcid Fusion
        bb_node_embed = self.node_fusion(bb_aa_embed)
        bb_node_embed = bb_node_embed * bb_mask[..., None]

        # Initialze Substrate Masking
        lig_mask = input_feats["ligand_mask"]
        lig_edge_mask = lig_mask[..., None] * lig_mask[..., None, :]
        # Encode Substrate with 3D Molecule GNN
        lig_init_node_embed, _ = self.mol_embedding_layer(
                ligand_atom=input_feats["ligand_atom"],
                ligand_pos=input_feats["ligand_pos"],
                edge_mask=lig_edge_mask,
            )
        lig_node_embed = lig_init_node_embed * lig_mask[..., None]

        # Backbone-Substrate Fusion
        bb_lig_rep, _ = self.bb_lig_fusion(
                                query_input=bb_node_embed,
                                key_input=lig_node_embed,
                                value_input=lig_node_embed,
                                query_input_mask=bb_mask,
                                key_input_mask=lig_mask,
                            )

        # Residue Connection
        bb_node_embed = bb_node_embed + bb_lig_rep

        # Conditioning on Product Molecule
        if self.condition_generation:
            # Encode Product with 2D Molecule GNN
            guide_ligand_rep = self.guide_ligand_mpnn(
                                mol_atom=input_feats["guide_ligand_atom"],
                                mol_edge=input_feats["guide_ligand_edge_index"],
                                mol_edge_feat=input_feats["guide_ligand_edge"],
                                mol_atom_mask=input_feats["guide_ligand_atom_mask"],
                                mol_edge_mask=input_feats["guide_ligand_edge_mask"],
                            ).unsqueeze(1)

            # Initialze Product Masking
            guide_ligand_mask = input_feats["guide_ligand_atom_mask"][:, 0:1]
            # Backbone-Product Fusion
            bb_guide_lig_rep, _ = self.guide_bb_lig_fusion(
                                    query_input=bb_node_embed,
                                    key_input=guide_ligand_rep,
                                    value_input=guide_ligand_rep,
                                    query_input_mask=bb_mask,
                                    key_input_mask=guide_ligand_mask,
                                )

            # Residue Connection
            bb_node_embed = bb_node_embed + bb_guide_lig_rep

        # Initialze Backbone-Substrate Masking
        bb_ligand_mask = torch.cat([bb_mask, lig_mask], dim=-1)
        # Backbone-Substrate Distance Embedding
        bb_lig_edge = self.edge_dist_embedder(
            rigid=input_feats["rigids_t"],
            ligand_pos=input_feats["ligand_pos"],
            bb_ligand_mask=bb_ligand_mask,
        )

        # Backbone-Backbone-Product Edge Fusion
        bb_edge_embed = bb_edge_embed + bb_lig_edge[:, :n_res, :n_res, :]

        # Masking Padded Residues
        bb_node_embed = bb_node_embed[:, :n_res, :] * bb_mask[..., None]
        bb_edge_embed = bb_edge_embed[:, :n_res, :n_res, :] * edge_mask[..., None]

        # Run IPA Network
        model_out = self.ipanet(bb_node_embed, bb_edge_embed, input_feats)
        node_embed = model_out["node_embed"] * bb_mask[..., None]

        # Amino Acid Prediction with Amino Acid Prediction Network
        aa_pred = self.aatype_pred_net(node_embed) * bb_mask[..., None]

        if self._model_conf.flow_msa:
            # Encode Coevo with Co-Evolution Embedder
            msa_mask = input_feats["msa_mask"]
            msa_embed = self.msa_embedding_layer(input_feats["msa_t"], msa_mask=msa_mask) *
    msa_mask[..., None] #[B, N_msa, N_token, D]
            msa_rep = msa_embed.sum(dim=1) / (msa_mask[..., None].sum(dim=1) + 1e-10) #[B, 1,
    D]
            _msa_mask = msa_mask[:, 0] #torch.ones_like(msa_rep[..., 0]).to(msa_embed.device)

            # Coevo-Backbone Fusion
            msa_rep, _ = self.msa_bb_lig_fusion(
                                        query_input=msa_rep,
                                        key_input=node_embed,
                                        value_input=node_embed,
                                        query_input_mask=_msa_mask,
                                        key_input_mask=bb_mask,
                                    )

            # Coevo Prediction with Coevo Prediction Network
            msa_pred = self.msa_pred(msa_rep)

        if self._model_conf.flow_ec:
            # Encode EC with EC Embedder
            ec_embed = self.ec_embedding_layer(input_feats["ec_t"])
            ec_mask = torch.ones_like(ec_embed[..., 0]).to(ec_embed.device)

            # EC-Backbone Fusion
            ec_rep, _ = self.ec_bb_lig_fusion(
                                    query_input=ec_embed,
                                    key_input=node_embed,
                                    value_input=node_embed,
                                    query_input_mask=ec_mask,
                                    key_input_mask=bb_mask,
                                )

            # EC Prediction with EC Prediction Network
            ec_rep = ec_rep.reshape(n_batch, -1)
            ec_pred = self.ec_pred(ec_rep)

        # Main Network Ouput
        pred_out = {
            "amino_acid": aa_pred,
            "rigids_tensor": model_out["rigids"],
        }

        if self._model_conf.flow_msa:
            pred_out["msa"] = msa_pred * _msa_mask[..., None]

        if self._model_conf.flow_ec:
            pred_out["ec"] = ec_pred

        pred_out["rigids"] = model_out["rigids"].to_tensor_7()
        return pred_out
```

Listing 4: Pytorch Implementation of EnzymeFlow Main Network.

Fun Fact: While implementing enzyme-substrate and enzyme-product interactions by cross-attention fusion networks, we experimented with using PairFormer (with only 3-4 layers) as implemented in AlphaFold3 (Abramson et al., 2024). However, the computational load was immense—it would take years to run on our A40 GPU. Our fusion network turns to be a more efficient approach. It makes me wonder who has the resources to re-train AlphaFold3, given the heavy computational demands!